European Journal of Medicinal Chemistry 159 (2018) 324–338

Contents lists available at ScienceDirect

European Journal of Medicinal Chemistry

journal homepage: http://www.elsevier.com/locate/ejmech

Research paper

1-(2-Hydroxybenzoyl)-thiosemicarbazides are promising antimicrobial agents targeting D-alanine-D-alanine ligase *in bacterio*

Alice Ameryckx [a, 1], Léopold Thabault [a, 1], Lionel Pochet [b], Serge Leimanis [c], Jacques H. Poupaert [a], Johan Wouters [d], Bernard Joris [c], Françoise Van Bambeke [e], Raphaël Frédérick [a, *]

[a] Medicinal Chemistry Research Group (CMFA), Louvain Drug Research Institute (LDRI), Université Catholique de Louvain (UCLouvain), 73 Avenue Mounier, B1.73.10, 1200, Bruxelles, Belgium
[b] Department of Pharmacy, Namur Medicine & Drug Innovation Center (NAMEDIC), Namur Research Institute for Life Sciences (NARILIS), University of Namur, Namur, Belgium
[c] Centre d'Ingénierie des Protéines, Institut de Chimie B6A, Sart-Tilman, Université de Liège, Liège, Belgium
[d] Department of Chemistry, Namur Medicine & Drug Innovation Center (NAMEDIC), Namur Research Institute for Life Sciences (NARILIS), University of Namur, Namur, Belgium
[e] Pharmacologie Cellulaire et moléculaire (FACM), Louvain Drug Research Institute (LDRI), Université Catholique de Louvain (UCLouvain), 73 Avenue Mounier, B1.73.05, 1200 Bruxelles, Belgium

ARTICLE INFO

Article history:
Received 4 May 2018
Received in revised form
9 August 2018
Accepted 26 September 2018
Available online 28 September 2018

Keywords:
D-alanine-D-alanine ligase inhibitors
Benzoylthiosemicarbazides
Antimicrobial agents
Antibiotics
Structure-activity relationships

ABSTRACT

The bacterial cell wall and the enzymes involved in peptidoglycan synthesis are privileged targets for the development of novel antibacterial agents. In this work, a series of 1-(2-hydroxybenzoyl)-thiosemicarbazides inhibitors of D-Ala-D-Ala ligase (Ddl) were designed and synthesized in order to target resistant strains of bacteria. Among these, the 4-(3,4-dichlorophenyl)-1-(2-hydroxybenzoyl)-3-thiosemicarbazide **29** was identified as a potent Ddl inhibitor with activity in the micromolar range. This compound, possessing strong antimicrobial activity including against multidrug resistant strains, was proven to act through a bactericidal mechanism and demonstrated very low cytotoxicity on THP-1 human monocytic cell line. Inhibition of Ddl activity by **29** was confirmed *in bacterio* using UPLC-MS/MS by demonstrating an increase in D-Ala intracellular pools accompanied by a commensurate decrease in D-Ala-D-Ala. Further structure-activity relationships (SARs) studies provided evidence that the hydroxyl substituent in the 2-position (R_1) of the benzoylthiosemicarbazide scaffold is essential for the enzymatic inhibition. This work thus highlights the 1-(2-hydroxybenzoyl)-thiosemicarbazide motif as a very promising tool for the development of novel antibacterial compounds acting through an interesting mechanism of action and low cytotoxicity.

1. Introduction

In an era of growing antibiotic resistance, the search for effective molecules with novel mechanisms of action is a priority [1]. Today, the bacterial cell wall and the enzymes involved in peptidoglycan biosynthesis, a major cell wall structural component, constitute validated targets of many antimicrobial agents [2]. The peptidoglycan is a polymeric network which alternates *N*-acetylglucosamine (Glc*N*Ac) and *N*-acetylmuramic acid (Mur*N*Ac) disaccharide units cross-linked via peptide bonds [3] thanks to the catalytic activity of D,D-transpeptidases. These enzymes catalyze the reticulation of the peptide chains ending in D-Ala-D-Ala, with subsequent elimination of the terminal D-Ala residue and transfer of the remaining peptide chain on the lateral amino group of another peptide of an adjacent glycan chain. This last step of peptidoglycan biosynthetic pathway is inhibited by β-lactams antibiotics (such as penicillins), which act as suicide inhibitors of the transpeptidases [4], and by glycopeptides (vancomycin) that directly bind the terminal D-Ala-D-Ala moiety, creating a steric hindrance that prevents the access of D,D-transpeptidases to their substrate [5]. However, the frequent resistance associated with the use of these antibiotics revealed the need to target other enzymes acting on earlier steps of

* Corresponding author.
E-mail address: raphael.frederick@uclouvain.be (R. Frédérick).
[1] AA and LT contributed equally to this work.

https://doi.org/10.1016/j.ejmech.2018.09.067
0223-5234/

peptidoglycan synthesis [6]. Among these, D-alanine-D-alanine ligase (Ddl) represents a very interesting target.

Ddl is present in both Gram-negative and -positive bacteria and catalyzes the formation of D-Ala-D-Ala dipeptide, an early step in peptidoglycan synthesis. Two isoforms exist for *E. coli* and *S. typhimurium*, DdlA and DdlB [7]. Alternative ligases, catalyzing the formation of D-Ala-D-Lac (VanA, −B and -D types) or D-Ala-D-Ser (VanC, -E, -G and -L types), were also described in vancomycin-resistant enterococci [5,8]. Therefore, the discovery of inhibitors that are active not only on Ddl but also on these alternative ligases would increase their potential spectrum of activity. Today, various crystallographic structures of DdlB in presence of inhibitors, or in the *apo* form, are available and could thus contribute to the rational development of novel antibiotics [9–12]. Over the past few years, four main classes of Ddl inhibitors were described [6]. First, analogues of the substrate D-Ala were reported [13–17] including D-cycloserine (DCS, Fig. 1), [18–21] the only inhibitor used in the past as a therapeutic agent. However, its use is rather limited due to its known neurotoxicity. [22] This cyclic analogue of D-Ala acts as a competitive and reversible inhibitor of Ddl ($K_i = 25$ μM against *M. tuberculosis* Ddl) [19] and exhibits relatively high MIC values (50 mg/L against *M. tuberculosis*) [23]. Secondly, compounds that mimic the transition state of the enzymatic reaction were reported. These latter inhibit Ddl by acting as false substrates. Interestingly, these compounds allowed crystallographic studies of the enzyme-inhibitor complex thus affording important structural information for drug design [24,25]. Third, analogues of the reaction product D-Ala-D-Ala also showed interesting Ddl inhibition [13,26]. Fourth, inhibitors showing no structural resemblance with the substrate, the reaction intermediate or the product were discovered by screening chemical libraries or by rational drug design [27–36]. For instance, thanks to a high-throughput screening against *S. aureus* Ddl (StaDDl), compound **1** (Fig. 1) was identified ($K_i = 4$ μM). Although modestly active, this compound was used in structural studies and revealed a novel binding mode at an allosteric site [12]. This study thus paves the way to the development of original Ddl inhibitors acting via new mechanisms of inhibition. However, even if the most potent molecules reported so far showed inhibitory potencies in the micromolar range, only a few of them were evaluated for their antibacterial activity, which unfortunately usually remained very low.

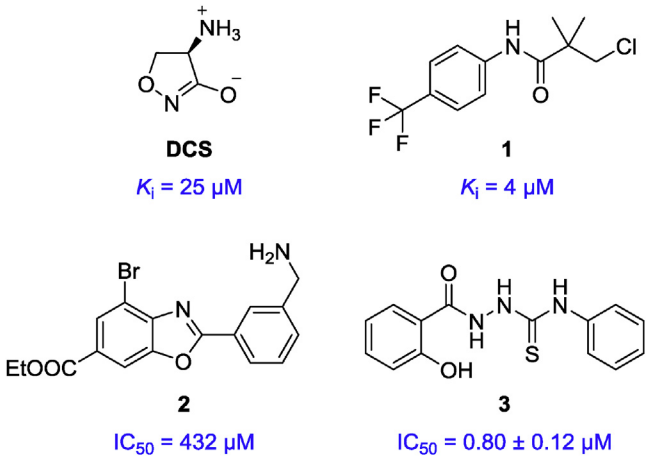

Fig. 1. Chemical structure and affinity for Ddl or inhibitory potency of DCS (*M. tuberculosis* Ddl) [19], 3-chloro-2,2-dimethyl-*N*-[4-(trifluoromethyl)phenyl]propanamide **1** (*S. aureus* Ddl) [12] and 2-phenylbenzoxazole **2** (*E. faecalis* Ddl) [33] reported in the literature. The IC_{50} of 1-(2-hydroxybenzoyl)-4-phenyl-3-thiosemicarbazide **3** (*E. faecalis* Ddl) is presented as the mean ± SD of experiments realized in triplicate, n = 2.

An initial *de novo* design study carried out previously in our group allowed identifying the 2-phenylbenzoxazole series, exemplified by molecule **2** (Fig. 1), as promising Ddl inhibitors. This series, however, revealed to be deprived of any antibacterial activity [33]. In the present work, we performed a screening of our internal library of compounds and identified the 1-(2-hydroxybenzoyl)-4-phenyl-3-thiosemicarbazide **3** (Fig. 1) as an interesting tool compound with an IC_{50} of 0.80 μM against Ddl (*E. faecalis*) and relatively weak but reasonable antimicrobial potency on *S. aureus* ATCC 25923 and *E. faecalis* ATCC 29212 with MIC values of 128 mg/L and 512 mg/L respectively. We found from the literature that this compound was, in fact, previously reported to be a very weak carbonic anhydrase inhibitor I and IX ($K_i > 80$ μM on both isoforms) [37] and to have some antibacterial activities evaluated against usual random strains, although no information were given regarding its mode of action [38]. These encouraging results prompted us to further develop and study this series of compounds, particularly their mode of action as antibacterials.

Various pharmacomodulations of compound **3** were investigated to improve the Ddl inhibition and the antibacterial potency, and to establish qualitative structure-activity relationships. The mechanism of action towards Ddl was also studied and the activity against Gram-positive and negative, sensitive or resistant strains to current therapeutics was determined. Finally, the *in vivo* biochemical mechanism was determined by UHPLC-MS/MS dosage of intracellular L-Ala, D-Ala and D-Ala-D-Ala levels in response to 4-(3,4-dichlorophenyl)-1-(2-hydroxybenzoyl)-3-thiosemicarbazide **29**.

2. Chemistry

The synthesis of benzoylthiosemicarbazides **3** and **14**–**49** was carried out according to a two-step procedure presented in Scheme 1. First, the benzohydrazides **4**–**13** were obtained according to the literature by refluxing hydrazine hydrate and the appropriate methyl benzoate in ethanol or were commercially available (**4** and **8**) [39,40]. Then, these benzohydrazides were reacted with various isothiocyanates in refluxing methanol or at room temperature [41,42]. The targeted benzoylthiosemicarbazides **3** and **14**–**49** were collected by filtration and recrystallized from ethanol if necessary.

The three labile protons (NH) of the thiosemicarbazide linker were visible on ^{1}H NMR in DMSO at approximately 9.72 ppm, 9.94 ppm and 10.47 ppm depending on the substituents of the thiosemicarbazide motif. The ^{1}H NMR spectrum of 1-(2-hydroxybenzoyl)-thiosemicarbazides **3**, **22**–**42** showed a duplication of two labile proton signals of the −NH−NH− functionality, probably reflecting an equilibrium between two of the potential tautomeric forms of this molecule (Scheme 2), as well as the 1-(2-methoxybenzoyl)-thiosemicarbazide **49** and the 1-(2-hydroxynaphtoyl)-thiosemicarbazide **51**. As this peak splitting can only be seen for the benzoylthiosemicarbazides bearing a substituent containing an oxygen in the 2-position (see Supporting Information), intramolecular H-bonding was suggested to explain this enol form stabilization allowing to observe both peaks in ^{1}H NMR. The existence of this keto-enol equilibrium for 1-(2-hydroxybenzoyl)-thiosemicarbazides was already mentioned in the literature [43].

To better understand the structure-activity relationships (SARs) in this series, other analogues were also prepared. First, the left part of the model compound **3** was rigidified by introducing a quinazolinone moiety and extended with the replacement of the phenyl by a naphtyl group, as depicted in Scheme 3. After obtaining the naphtohydrazide precursor **50**, the syntheses of **51**–**52** were thus carried out following the previous procedure for thiosemicarbazides synthesis. We then also investigated the replacement of the thiocarbonyl

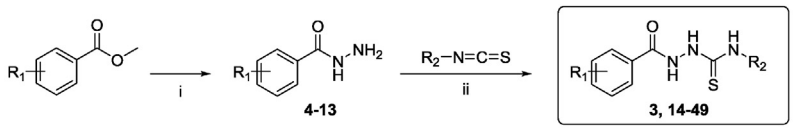

4 R_1 = H
5 R_1 = 2-OH
6 R_1 = 3-OH
7 R_1 = 4-OH
8 R_1 = 2-F
9 R_1 = 3-F
10 R_1 = 4-F
11 R_1 = 2-OH-4-I
12 R_1 = 2-OH-4-NH_2
13 R_1 = 2-OMe

14 R_1 = H, R_2 = Ph
15 R_1 = H, R_2 = 2-ClPh
16 R_1 = H, R_2 = 3-ClPh
17 R_1 = H, R_2 = 4-ClPh
18 R_1 = H, R_2 = 2-FPh
19 R_1 = H, R_2 = 3-FPh
20 R_1 = H, R_2 = 4-FPh
21 R_1 = H, R_2 = 3,4-diClPh
3 R_1 = 2-OH, R_2 = Ph
22 R_1 = 2-OH, R_2 = 2-ClPh

23 R_1 = 2-OH, R_2 = 3-ClPh
24 R_1 = 2-OH, R_2 = 4-ClPh
25 R_1 = 2-OH, R_2 = 2-FPh
26 R_1 = 2-OH, R_2 = 3-FPh
27 R_1 = 2-OH, R_2 = 4-FPh
28 R_1 = 2-OH, R_2 = 2,4-diClPh
29 R_1 = 2-OH, R_2 = 3,4-diClPh
30 R_1 = 2-OH, R_2 = 2-OMePh
31 R_1 = 2-OH, R_2 = 4-OMePh
32 R_1 = 2-OH, R_2 = 4-CNPh

33 R_1 = 2-OH, R_2 = n-Pentyl
34 R_1 = 2-OH, R_2 = 3-Morpholinopropyl
35 R_1 = 2-OH, R_2 = 1-Naphtyl
36 R_1 = 2-OH, R_2 = 3-IPh
37 R_1 = 2-OH, R_2 = 4-AcetylPh
38 R_1 = 2-OH, R_2 = 4-OCF_3Ph
39 R_1 = 2-OH, R_2 = 4-BenzyloxyPh
40 R_1 = 2-OH, R_2 = 3-Pyridinyl
41 R_1 = 2-OH-4-I, R_2 = 3,4-diClPh
42 R_1 = 2-OH-4-NH_2, R_2 = 3,4-diClPh

43 R_1 = 3-OH, R_2 = 3,4-diClPh
44 R_1 = 4-OH, R_2 = 3,4-diClPh
45 R_1 = 4-OH, R_2 = 4-NO_2Ph
46 R_1 = 2-F, R_2 = 3,4-diClPh
47 R_1 = 3-F, R_2 = 3,4-diClPh
48 R_1 = 4-F, R_2 = 3,4-diClPh
49 R_1 = 2-OMe, R_2 = 3,4-diClPh

Scheme 1. Synthetic route for the preparation of the benzoylthiosemicarbazides **3** and **14**–**49** and their precursors **4**–**13**.[aa] Reagents and conditions: (i) 65% hydrazine hydrate (5 equiv), EtOH, reflux, 2.5 h-24 h (ii) MeOH, reflux or r.t., 0.5 h-24 h.

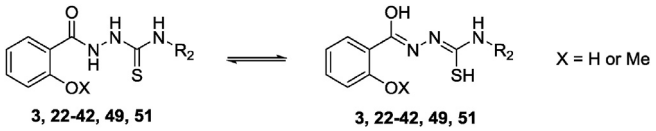

Scheme 2. Potential keto-enol equilibrium for compounds bearing a substituent containing an oxygen in the 2-position is visible in ^{1}H NMR spectrum.

moiety by a carbonyl group to obtain the semicarbazide motif. To this end, the commercially available benzohydrazide **4** and 2-hydroxybenzohydrazide **5** were added to 3,4-dichloro isocyanate in methanol at reflux to afford respectively 2-benzoyl-*N*-(3,4-dichlorophenyl)hydrazine-1-carboxamide **53** and *N*-(3,4-dichlorophenyl)-2-(2-hydroxybenzoyl)hydrazine-1-carboxamide **54** (Scheme 3) following the adapted known procedure [44].

The structures and purities were assessed by ^{1}H NMR, ^{13}C NMR, HRMS and HPLC. The analysis of spectral data of the target compounds are provided in the experimental section. These molecules were subsequently evaluated on Ddl using purified *His*-tagged Ddl and their antimicrobial activity was assessed on sensitive and resistant bacteria.

3. Pharmacological evaluation and discussion

3.1. Enzymatic assay

3.1.1. Optimization

Prior to the evaluation of compounds **3**, **14**–**49** and **51**–**54** towards recombinant *His*-tagged Ddl from *E. coli*, the colorimetric malachite green assay [45] was optimized for the determination of inorganic phosphate generated during the reaction catalyzed by Ddl. The linearity zone (Fig. 2a), the optimal working conditions (Fig. 2b), the tolerance to DMSO (Fig. 2c) and the K_m values for the two D-Ala sites (Fig. 2d) were determined. The linearity zone for

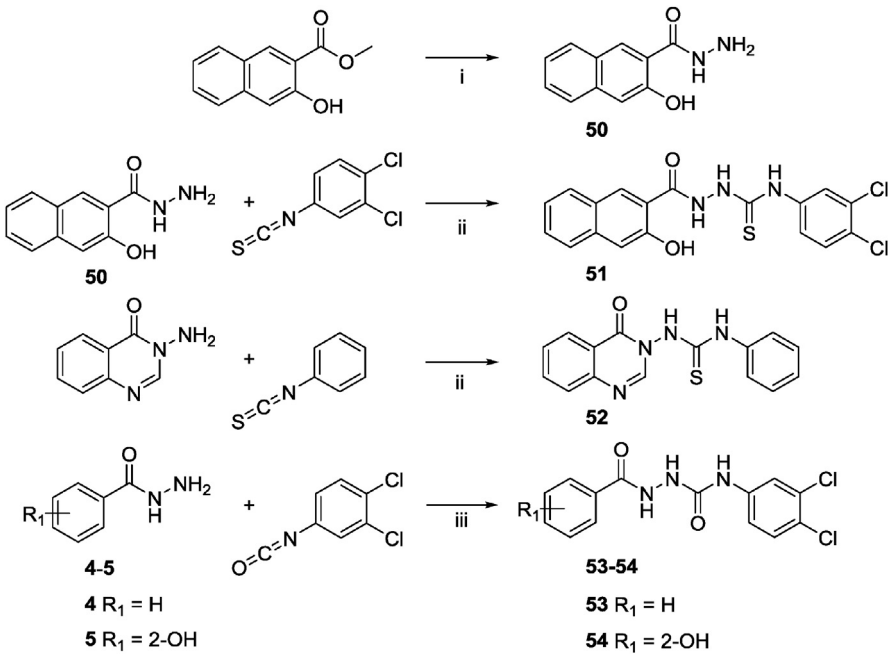

Scheme 3. Synthesis of new structural analogues. [aa] Reagents and conditions: (i) 65% hydrazine hydrate (5 equiv), EtOH, reflux, 1 h (ii) EtOH, reflux, 4 h- 20 h (iii) MeOH, reflux, 17 h.

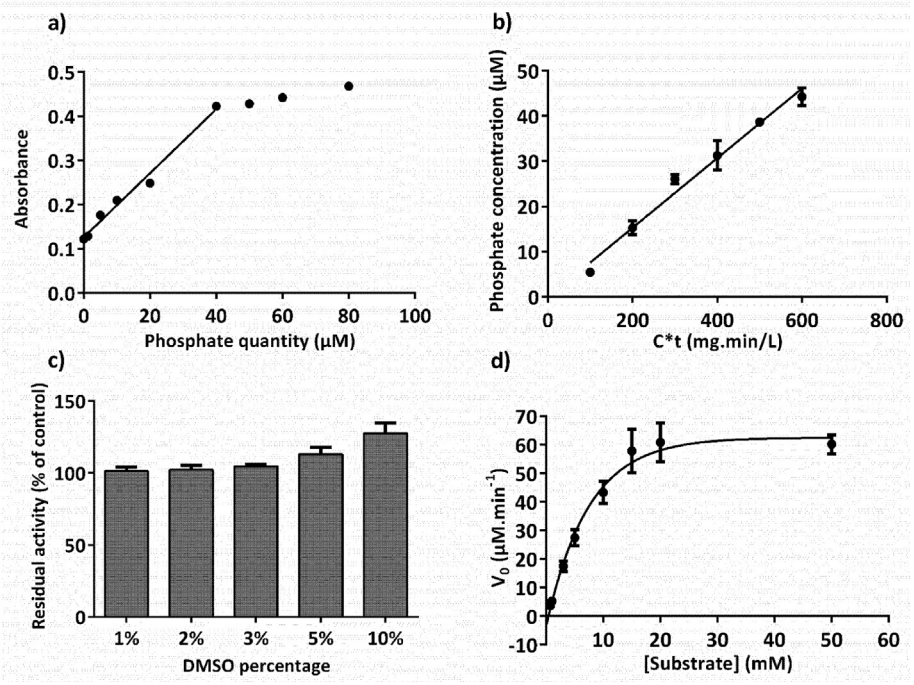

Fig. 2. Optimization of the enzymatic assay. D-Ala and ATP concentrations were set respectively at 1 mM and 500 µM. Buffer composition was 20 mM Tris.HCl (pH 7.4), 10 mM $MgCl_2$, 10 mM KCl. **(a)** Evolution of the absorbance as a function of phosphate concentrations in µM. Inorganic phosphate (0–80 µM) was incubated with malachite green for 25 min. Absorbance was monitored at 650 nm. **(b)** Evolution of phosphate concentration (µM) in relationship with the product of enzyme concentration (mg/L) and time (min). Concentrations of Ddl were 5–20 mg/L. Incubation time with the substrate was 0–30 min. **(c)** Evaluation of DMSO influence on the enzymatic activity. DMSO concentrations (v/v) were 1, 2, 3, 5 and 10%. **(d)** Velocity of the enzyme (µM.min^{-1}) as a function of substrate concentration (mM). Substrate concentrations were 0.45–30 fold the theoretical K_{m2} (value reported in the literature) [7,46]. Apparent $K_m = 5.62$ mM.

the phosphate concentrations is from 0 to 40 µM. Working conditions are 20 min of incubation time with D-Ala, 20 mg/L of enzyme concentration and 10% of DMSO. A detailed description of the assay optimization can be found in the Supporting Information.

3.1.2. Activity of inhibitors on the purified enzyme

A primary screening at 10 µM ([D-Ala] = 1 mM) was performed in triplicate to select inhibitors that lowered the Ddl activity of 30% or more (Ddl inhibition ≥ 30%). Then, for the most active compounds, an IC_{50} was determined after 30 min of incubation with Ddl (Table 1). DCS was used as a reference and it showed an IC_{50} of 262 µM in our hands, similar to the published data [6].

Firstly, compared to the parent compound **3**, it can be observed that removal of the hydroxyl group in the 2-position always leads to inactive compounds (**14**–**21**), independently of the nature of the substituent present on the right part (R_2) of the molecule (Table 1). When this hydroxyl group is replaced by a bioisosteric fluorine **46**–**48** (R_1 = F) or a methoxyl group **49** (R_1 = OMe), no inhibition is found either. Further comparison of the hydroxybenzoylthiosemicarbazides **29**, **43** and **44** possessing the hydroxyl function in the 2-, 3- and 4-position, respectively, also clearly reveals that only the 2-position is tolerated. However, it seems that an additional substituent on the left phenyl (**41**–**42**), or its replacement by a naphtyl group (**51**), allows to keep the activity if the 2-OH is still present. This feature indicates that there is still enough space in the inhibitor binding pocket and could be important for further structural modifications.

It thus appears from these first SAR modifications that a hydroxyl group in this 2-position is key for Ddl inhibition. Because its replacement by a fluorine leads to inactive compounds, it may be inferred that (i) it probably contributes to the stabilization of the inhibitor inside the Ddl cavity through H-bonding with residues bearing H-bond acceptor groups and (ii) it could stabilize a particular conformation by intramolecular H-bonding. This hypothesis was further validated by the X-ray structure of a representative benzoylthiosemicarbazide **29**. As observed from Fig. 3, this compound co-crystallized with one DMSO molecule from the crystallization solvent. The analysis of the X-ray structure of **29** revealed that the hydroxyl group on the aromatic ring was, as suggested, intramolecularly H-bonded to the thiosemicarbazide NH (N–H•••O interaction) leaving the OH available for an additional intermolecular H-bond with the DMSO sulfoxide function. The OH group in the 2-position thus probably plays a key role both as an intramolecular H-bond acceptor and an intermolecular H-bond donor. The inactivity of compound **49** bearing a 2-methoxy substituent reinforces this hypothesis.

Thereafter, we investigated the effect of the modulation on the right part (R_2) of the benzoylthiosemicarbazide scaffold. In this position an electron-withdrawing (Cl, F, CN, I …) or electron-donating (MeO, BnO …) substituent is introduced at the phenyl ring (**22**–**32** and **36**–**39**). Subsequent Ddl inhibition is always in the same range to that of the parent compound **3** (in the submicromolar range). Interestingly, the introduction of a pentyl (**33**) or a naphtyl (**35**) group in the same position also leads to potent Ddl inhibitors, in similar range that previously tested molecules. On the contrary, introduction of more hydrophilic substituents such as 3-morpholinopropyl (**34**) or pyridin-3-yl (**40**) decreases the Ddl inhibition as this compound exhibits only a maximum Ddl inhibition of 30% at the highest concentration. The data obtained thanks to these pharmacomodulations on R_2 suggest that no critical interaction is made between this part of the molecule and the enzymatic cavity apart from hydrophobic interactions.

Finally, the importance of the thiosemicarbazide linker was assessed. Its replacement by a semicarbazide function, with (**54**) and without (**53**) the hydroxyl substituent in the 2-position of the aromatic ring (R_1), as well as the complete replacement of the 4-

Table 1
Structures, Ddl inhibitory activities and some physicochemical parameters of compounds **3**, **14**–**49** and **51**–**54**.

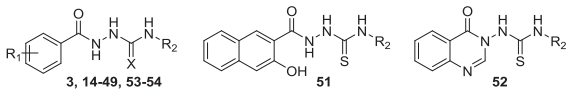

Compd	X	R_1	R_2	IC_{50} (μM)[a]	LogD[b] (pH = 7.4)	TPSA[b]	S (mmol/L)[b] (pH = 7.4)
3	S	2-OH	Phenyl	0.80 ± 0.12	2.31	105.48	0.94
14	S	H	Phenyl	n.a.	2.14	85.25	0.82
15	S	H	2-Chlorophenyl	n.a.	2.63	85.25	0.2
16	S	H	3-Chlorophenyl	n.a.	2.87	85.25	0.07
17	S	H	4-Chlorophenyl	n.a.	2.69	85.25	0.05
18	S	H	2-Fluorophenyl	n.a.	2.17	85.25	0.5
19	S	H	3-Fluorophenyl	n.a.	2.37	85.25	0.3
20	S	H	4-Fluorophenyl	n.a.	2.19	85.25	0.26
21	S	H	3,4-Dichlorophenyl	n.a.	3.57	85.25	0.002
22	S	2-OH	2-Chlorophenyl	0.79 ± 0.14	2.79	105.48	0.31
23	S	2-OH	3-Chlorophenyl	0.63 ± 0.13	3.13	105.48	0.07
24	S	2-OH	4-Chlorophenyl	0.83 ± 0.16	2.87	105.48	0.12
25	S	2-OH	2-Fluorophenyl	0.97 ± 0.18	2.22	105.48	0.46
26	S	2-OH	3-Fluorophenyl	0.10 ± 0.15	2.50	105.48	0.25
27	S	2-OH	4-Fluorophenyl	0.84 ± 0.17	2.28	105.48	0.23
28	S	2-OH	2,4-Dichlorophenyl	0.58 ± 0.15	3.40	105.48	0.04
29	S	2-OH	3,4-Dichlorophenyl	1.54 ± 0.30	3.63	105.48	0.008
30	S	2-OH	2-Methoxyphenyl	0.55 ± 0.08	2.36	114.71	0.65
31	S	2-OH	4-Methoxyphenyl	0.71 ± 0.13	2.18	114.71	0.72
32	S	2-OH	4-Cyanophenyl	0.51 ± 0.11	2.02	129.27	0.64
33	S	2-OH	Pentyl	0.93 ± 0.15	2.75	105.48	0.32
34	S	2-OH	3-Morpholinopropyl	[c]	0.71	117.95	13.4
35	S	2-OH	1-Naphthyl	0.52 ± 0.14	3.37	105.48	0.08
36	S	2-OH	3-Iodophenyl	0.73 ± 0.12	3.23	105.48	0.03
37	S	2-OH	4-Acetylphenyl	0.37 ± 0.04	2.08	122.55	0.47
38	S	2-OH	4-Trifluoromethoxyphenyl	0.70 ± 0.16	2.89	114.71	0.08
39	S	2-OH	4-Benzyloxyphenyl	0.99 ± 0.99	3.54	114.71	0.04
40	S	2-OH	Pyridin-3-yl	[c]	1.32	118.37	3.82
41	S	2-OH-4-I	3,4-Dichlorophenyl	0.93 ± 0.12	4.31	105.48	0.007
42	S	2-OH-4-NH_2	3,4-Dichlorophenyl	0.99 ± 0.99	3.01	131.5	0.009
43	S	3-OH	3,4-Dichlorophenyl	n.a.	3.30	105.48	0.01
44	S	4-OH	3,4-Dichlorophenyl	n.a.	3.25	105.48	0.01
45	S	4-OH	4-Nitrophenyl	n.a.	1.89	154.31	0.45
46	S	2-F	3,4-Dichlorophenyl	n.a.	3.26	85.25	0.003
47	S	3-F	3,4-Dichlorophenyl	n.a.	3.49	85.25	0.003
48	S	4-F	3,4-Dichlorophenyl	n.a.	3.50	85.25	0.003
49	S	2-OMe	3,4-Dichlorophenyl	n.a.	4.08	62.39	0.001
51	/	/	3,4-Dichlorophenyl	0.56 ± 0.07	4.54	105.48	0.0001
52	/	/	Phenyl	n.a.	1.95	88.82	0.75
53	O	H	3,4-Dichlorophenyl	n.a.	3.00	70.23	0.002
54	O	2-OH	3,4-Dichlorophenyl	n.a.	3.66	90.46	0.01
DCS	/	/	/	262 ± 43.4	/	/	/

n.a. = not active; 100% residual activity at 10 μM.
[a] IC_{50} values are presented as the (mean ± SD) of measures performed in triplicate ($n \geq 2$).
[b] LogD, TPSA (topological polar surface area) and S (solubility) were calculated with ACD/Labs® program.
[c] Ddl inhibition of 30% at 10 μM.

phenylthiosemicarbazide in **3** with a 1-(4-oxoquinazolin-3(4H)-yl) thiourea scaffold (**52**), to evaluate a cyclized structure, afford inactive derivatives.

Furthermore, according to the literature, the inhibition of Ddl by compound **3**, chosen for its good aqueous solubility, was tested in the presence and absence of 0.01% Triton X-100 to double-check that the activity was not an artefact due, for instance, to drug aggregation [47,48]. No change in Ddl inhibition was noticed, therefore proving that the activity was the result of a specific interaction to Ddl.

These results highlight the importance of the thiosemicarbazide template and the 2-OH benzoyl group for the proper recognition inside the Ddl enzyme cavity.

3.1.3. Study of the binding mode. A residual activity of Ddl of about 25% was always observed for active compounds after 30 min of incubation with the inhibitor. To gain a deeper understanding of the mechanism of action in this series a detailed study of the binding mode was investigated. Compound **3** was selected for its good aqueous solubility and adequate lipophilicity (Table 1). First, upon increasing the incubation time of the inhibitor with the enzyme from 10 to 120 min (Fig. 4a), we first noticed that, although the IC_{50} of **3** was not modified, the maximum inhibition percentage increased from 60% (10 min incubation) up to more than 90% (90 min incubation). Then, the reversibility of the inhibition was assessed using a rapid dilution assay [49]. To this end, **29** was selected as a model compound for subsequent studies given its activity on Ddl and bacteria (see below). As observed from Fig. 4b, the enzymatic activity was recovered after a rapid and large dilution of the enzyme-inhibitor complex, thus proving the reversible interaction of our inhibitors with Ddl.

Next, competition studies were carried out with **29** against both D-Ala and ATP (Fig. 5a and b). Regarding competition against D-Ala,

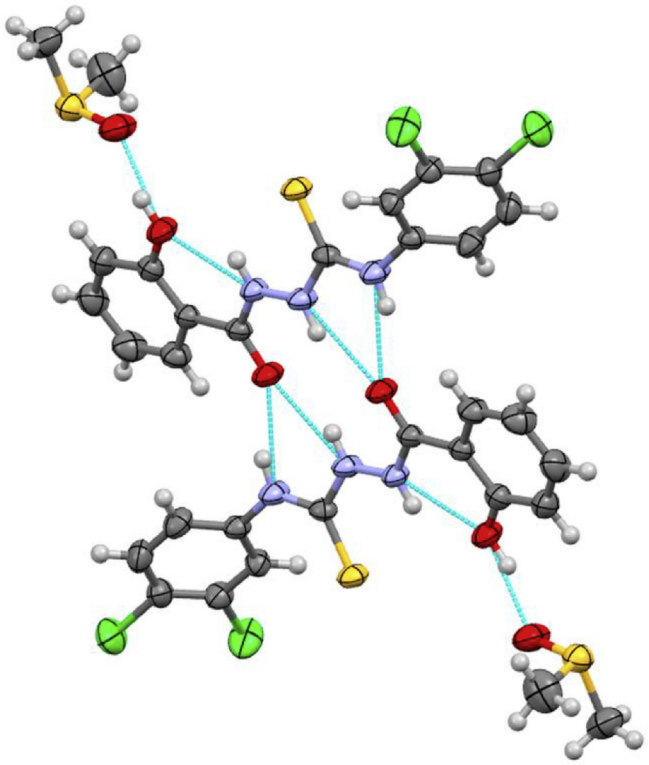

Fig. 3. View of the molecular interaction (H-bonds represented as dashed lines) within the crystal packing of compound **29** (ORTEP representation for each molecule, 50% probability representation).

as Ddl binds two D-Ala molecules in two distinct binding sites [50], we assumed that, at concentrations where the substrate occupies both sites (1 mM ~ K_{m2}), K_{m1} is negligible compared to K_{m2} [15,46]. When a saturating concentration of ATP (500 μM) was used, two K_m values for D-Ala were found (K_{m1} = 487.2 μM and K_{m2} = 10.5 mM). When a concentration of D-Ala of 50 mM was used, a K_m value for ATP of 691 μM could be approximated. Detailed information regarding these measurements can be found in the available Supporting Information.

Upon increasing concentrations of **29**, a decrease of the V_{max} value was observed on both graphs (Fig. 5). Moreover, we noticed that the V/K_m value also changes with increasing concentrations of **29** (see Supporting Information) thus suggesting a mixed non-competitive inhibition profile for this compound towards both D-Ala (α > 1, inhibitor preferentially binds the free enzyme) and ATP (α < 1, inhibitor preferentially binds the enzyme-ATP complex). This mechanism of action led us to hypothesize an interaction of **29** at an allosteric site rather than at the active site. This assumption is further supported by the recent identification of such an allosteric site on Ddl together with the identification of Ddl inhibitors with similar kinetic profile [12].

3.2. Biological activities

3.2.1In vitro antibacterial activity

The MICs of compounds **3**, **14**–**48** and **51**–**54** against two Gram-positive bacterial strains, *S. aureus* ATCC 25923 and *E. faecalis* ATCC 29212 were determined using maximal concentrations of 100 μM and 400 μM respectively (see details in the Supporting Information available) with 1% DMSO (v:v). Unfortunately, compounds **46**–**48** were not soluble at these concentrations. The most active compounds are **28** with a MIC of 50 μM (17.81 mg/L) against both strains, **29** with a MIC of 100 μM (35.62 mg/L) and 50 μM (17.81 mg/L) against *S. aureus* ATCC 25923 and *E. faecalis* ATCC 29212 respectively, **37**–**38** with MICs of 25 μM (8.23 and 9.28 mg/L) against *S. aureus* ATCC 25923 and 50 μM (16.47 and 18.56 mg/L) against *E. faecalis* ATCC 29212, and, finally, **40** with a MIC of 50 μM (14.42 mg/L) against both strains (Table 2). The benzoylthiosemicarbazides **22**–**27**, **32**, **39** and **41** have MICs ranging from 100 μM to 400 μM. In fact all these molecules have better *in vitro* activities than DCS, the reference antibiotic targeting Ddl. The other compounds assayed showed no biological activities at these concentrations.

The active compounds on Ddl, **3**, **22**–**42** and **51** were also assayed against various Gram-positive and negative bacteria, including clinical isolates resistant to current antibiotics and strains expressing alternative ligases (*E. faecalis* JH2-2::C1 [51], BM 4390 [52], BM 4575 [53]). MICs are shown in Table 3.

All the tested compounds were inactive against Gram-negative bacteria (*Klebsiella pneumoniae* ATCC 700603, *Escherichia coli* ATCC 25922 and *Pseudomonas aeruginosa* PAO1). Compound **28** was equipotent against all Gram-positive strains, including those expressing alternative ligases (*E. faecalis* BM 4390, BM 4575, JH2-2::C1; VRSA VRS-1) or resistant to glycopeptides, oxazolidinones, or fluoroquinolones, with MICs of 25–50 μM. The benzoylthiosemicarbazide **29** showed MICs of 50–100 μM, whatever the strain tested. Compound **22** displayed MIC of 100 μM towards *S. aureus* NRS 119, SA 325, SA 481 and VRS-1, and compound **23** showed MIC of 100 μM towards *S. aureus* SA 325, but these latter were not active on *E. faecalis* and the other staphylococci at 100 μM.

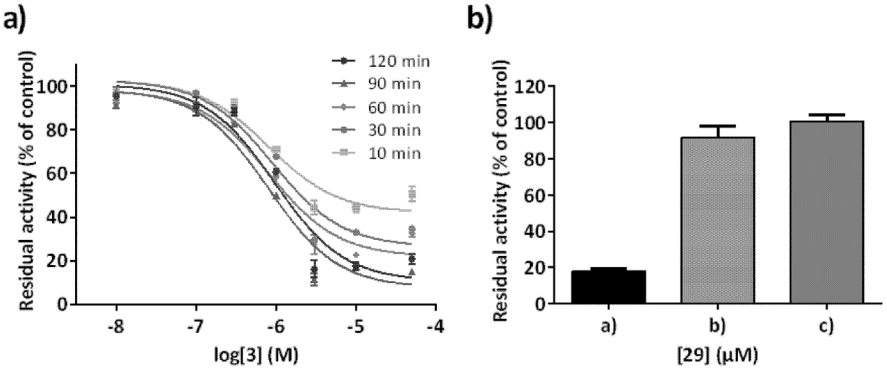

Fig. 4. **(a)** IC_{50} of benzoylthiosemicarbazide **3** with increasing incubation time (10, 30, 60, 90 and 120 min) of Ddl with the inhibitor. **(b)** Rapid dilution method with a) 3 μM of **29** and 200 mg/L of Ddl-His_6; b) 0.3 μM of **29** and 20 mg/L of Ddl-His_6 and c) rapid dilution of a) allows for the recovery of the activity compared to the control b). All values are presented as the (mean ± SD) of measures performed in triplicate.

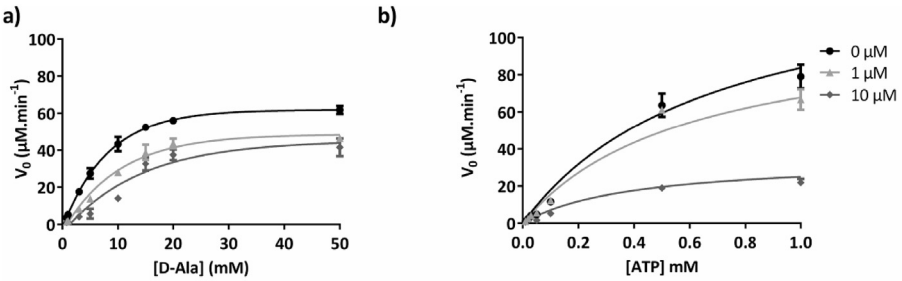

Fig. 5. Competition studies of model inhibitor **29** at three concentrations (0 µM, 1 µM and 10 µM) with **(a)** D-Ala: enzyme velocity (µM.min^{-1}) as a function of [D-Ala] (mM). **(b)** ATP: enzyme velocity (µM.min^{-1}) as a function of [ATP] (mM). All values are presented as the (mean ± SD) of measures performed in triplicate.

Table 2
MIC values of active benzoylthiosemicarbazides against fully susceptible Gram-positive reference strains.

Compd	MIC (mM/(mg/L))			
	S. aureus ATCC 25923[a]		*E. faecalis* ATCC 29212[a]	
	mM	mg/L	mM	mg/L
22	>0.1	>32.18	0.4	128.72
23	0.1	32.18	0.4	128.72
25	>0.1	>30.53	0.2	61.06
26	>0.1	>30.53	0.2	61.06
27	>0.1	>30.53	0.2	61.06
28	0.05	17.81	0.05	17.81
29	0.1	35.62	0.05	17.81
32	>0.1	>31.23	0.1	31.23
37	0.025	8.23	0.05	16.47
38	0.025	9.28	0.05	18.56
39	0.1	39.34	>0.4	>157.38
40	0.05	14.42	0.05	14.42
41	0.1	48.21	>0.4	>192.85
DCS	0.313	32	1.25	128

[a] *Staphylococcus aureus*, *S. aureus*; *Enterococcus faecalis*, *E. faecalis*.

Finally, compound **38** displayed MIC of 100 µM for *E. faecalis* JH2-2::C1, *S. aureus* NRS 119 and SA 325. These data suggest that compounds **28**, **29** and **38** may also be active on alternative ligases. Moreover, the ability of 2-hydroxybenzoyl-thiosemicarbazides derivatives to prevent the growth of various bacterial strains resistant to a wide range of antibiotics such as methicillin, linezolid, erythromycin, ciprofloxacin and moxifloxacin highlights them as attractive molecules warranting further development.

Interestingly, none of the benzoylthiosemicarbazides that are inactive on ligase exhibits antibacterial activity (see data in the Supporting Information). This supports our hypothesis that Ddl is the bacterial target of these compounds and could explain in part the antibacterial activity reported previously by other groups for benzoylthiosemicarbazide analogues [38,55,56]. Particularly, Siwek et al. and Plech et al. recently reported that 4-benzoylthiosemicarbazides derivatives could act as topoisomerase IV and DNA gyrase inhibitors [57,58]. However, no convincing concordance was found in their work between the antimicrobial activity and the inhibition of their presumed targets. The present analysis may therefore suggest that Ddl could be the bacterial target of these derivatives.

3.2.1. *Killing curve for compound **29***

To determine if the model compound **29** was bactericidal, killing curves were performed over 24 h for *S. aureus* ATCC 25923 exposed to increasing concentrations of inhibitor. As shown in Fig. 6, a bactericidal effect was reached when using a 10^6 CFU/mL starting inoculum after 24 h of incubation with concentrations of 2 or 5 × the MIC (0.2 and 0.5 mM), suggesting that the compound is slowly bactericidal. A complete eradication of bacteria was obtained at 5 × MIC.

*3.2.3. Determination of in vivo L-Ala, D-Ala and D-Ala-D-Ala levels in presence of model compound **29**.* In order to demonstrate that Ddl is effectively the *in vivo* biochemical target of our 1-(2-hydroxybenzoyl)-thiosemicarbazides, the effect of **29** on

Table 3
MIC values of active compounds **3**, **22**–**42** and **51** against Gram-positive resistant strains.

Compd	MIC (mM/(mg/L)) of:							
	E. faecalis[a]			*S. aureus*[b]				
	BM 4390	JH2-2::C1	BM 4575	MU 50	NRS 119	SA 325	SA 481	VRS-1
22	>0.1	>0.1	>0.1	>0.1	0.1/32.18	0.1/32.18	0.1/32.18	0.1/32.18
23	>0.1	>0.1	>0.1	>0.1	>0.1	0.1/32.18	>0.1	>0.1
28	0.025/8.90	0.05/17.81	0.025/8.90	0.05/17.81	0.025/8.90	0.05/17.81	0.05/17.81	0.025/8.90
29	0.05/17.81	0.1/35.62	0.05/17.81	0.1/35.62	0.05/17.81	0.05/17.81	0.1/35.62	0.05/17.81
38	>0.1	0.1/37.12	>0.1	>0.1	0.1/37.12	0.1/37.12	>0.1	>0.1
VAN[c]	0.7/**1024**	0.35/**512**	N.D.	0.005/**8**	0.0007/1	N.D.	N.D.	>0.175/>**256**
LZD[c]	N.D.	N.D.	N.D.	0.003/**1**	0.19/**64**	N.D.	N.D.	N.D.
CIP[c]	N.D.	N.D.	N.D.	N.D.	N.D.	N.D.	0.77/**256**	N.D.

[a] VRE (Vancomycin resistant *enterococcus*): *E. faecalis* BM 4390[52] (*vanB* genotype, *in vitro* mutant of a clinical isolate with inactive Ddl; constitutive expression of D-Ala-D-Lac); *E. faecalis* JH2-2::C1[51](*vanB* genotype, engineered derivative of JH2-2; constitutive expression of Ddl and of the VanB ligase); *E. faecalis* BM 4575[53] (*vanE* genotype, clinical isolate, constitutive expression of Ddl and of the VanE D-Ala-D-Ser ligase).

[b] *S. aureus* MU 50: MRSA (methicillin resistant *S. aureus*) and VISA (vancomycin intermediate resistant *S. aureus*); *S. aureus* NRS 119: MRSA resistant to linezolid (clinical isolate) [54]; *S. aureus* SA 325: CA-MRSA (community-acquired MRSA) resistant to erythromycin; *S. aureus* SA 481: HA-MRSA (hospital-acquired MRSA) resistant to ciprofloxacin and moxifloxacin; VRS-1: VRSA (vancomycin resistant *S. aureus*, *vanA* genotype) and HA-MRSA.

[c] VAN, vancomycin; LZD, linezolid; CIP, ciprofloxacin.

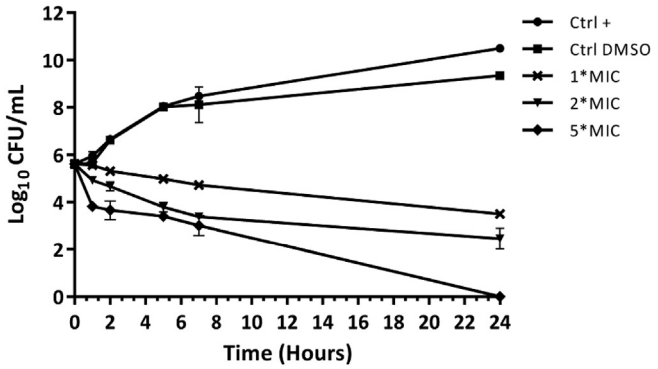

Fig. 6. Time-kill curves of *S. aureus* ATCC 25923 incubated with the model inhibitor **29**. The strain was incubated with growth media (●) as positive control, with 5% DMSO (■) as growth control; with molecule **29** at 1 × the MIC (×), 2 × the MIC (▼), and 5 × the MIC (◆). All values are presented as the (mean ± SD) of measures performed in triplicate.

intracellular levels of L-Ala, D-Ala and D-Ala-D-Ala was evaluated by UHPLC-MS/MS. To this end we used an LC-MS/MS methodology adapted from the literature in order to quantify these metabolites *in vivo* [17,59,60]. Briefly, the strategy involves the derivatization of L-Ala, D-Ala and D-Ala-D-Ala with Marfey's reagent [61] on *S. aureus* extracts followed by the chromatographic separation and detection of Marfey's derivatives in positive electrospray ionization (ESI) mode with multiple reaction monitoring (MRM) for the transition corresponding to a neutral loss of 45 Da $[M + H\text{-}45]^+$, the Marfey's terminal protonated amide. Based on preliminary experiments, we chose to expose bacteria to 2 × MIC of **29** for limited periods of time, i.e. conditions where only a modest decrease in bacterial counts was observed (Δ log CFU/mL = 1). The metabolite levels (L-Ala, D-Ala and D-Ala-D-Ala) were analyzed over 30 min.

As shown in Fig. 7, the [D-Ala]/[D-Ala-D-Ala] ratio increased over time in these conditions. This experiment thus proves that 1-(2-hydroxybenzoyl)-thiosemicarbazides exert their antimicrobial activity by targeting Ddl *in bacterio*.

3.2.2. Cytotoxicity of model compound *29*

The representative inhibitor **29** was then assayed for its potential cytotoxicity on THP-1 human monocytic cell line. Fig. 8 shows the evolution of cell survival as a function of time and inhibitor concentration. A significant but moderate (12–25%) decrease in viability was observed after 24 h of incubation over the range of concentrations investigated. This suggests that the compound is well tolerated at the concentrations showing antibacterial activity (1 × MIC or 0.1 mM).

*3.2.5. Selectivity profile of **29**.* Finally, these encouraging results prompted us to investigate the selectivity of **29**. To this effect, we tested its inhibitory activity against various enzymes and receptors at 10 μM, i.e. a concentration approx. 7 times higher than its IC_{50} towards Ddl (Table 4). From these data we can conclude that the 4-(3,4-dichlorophenyl)-1-(2-hydroxybenzoyl)-3-thiosemicarbazide **29** is highly selective for Ddl as none of the investigated enzymes or receptors are impacted in these conditions apart from the angiotensin converting enzyme, ACE, that is weakly inhibited (66%) by this compound. Despite that the literature describes the parent benzoylthiosemicarbazide **3** as a CA I and CA IX inhibitor, carbonic anhydrase II was not impacted by **29**.

These results demonstrate that the benzoylthiosemicarbazide motif is a selective and efficient pharmacological tool to target Ddl.

3.3. Molecular docking

Because the binding mode of **29** was established to be non-competitive, we performed a preliminary molecular docking study at the known allosteric site of Ddl. To this end, we used the structure of StaDdl available in the Protein Databank (PDB code: 2I80)[12] and docked **29** by mean of the automated Gold program with the aim to understand at the molecular level the interactions stabilizing the benzoylthiosemicarbazide in Ddl. To be consistent with the potential existence of tautomeric forms in this series of compounds, both tautomers of the model benzoylthiosemicarbazide **29** were investigated.

As a result, the binding mode of **29** in both tautomeric forms (Fig. 9a) supports the hypothesis that the right part of the inhibitor (R_2) could partially occupy a hydrophobic pocket (color code in green) open to the substrate binding site, and that no crucial interaction is made by this aromatic moiety apart from stabilizing hydrophobic interactions. At the bottom of the allosteric site, a quadrupolar T-shape interaction between Phe313 and the phenol ring of **29** ensures an additional stabilization. Moreover, it can be

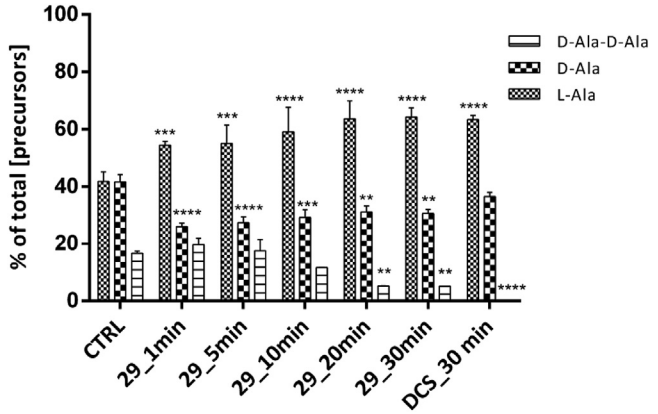

Fig. 7. Evolution over time of *S. aureus* L-Ala, D-Ala and D-Ala-D-Ala levels in presence of 2 × MIC of compound **29** compared to the control (DMSO 5%) and the reference antibiotic, DCS (2 × MIC). All values are presented as the (mean ± SD) of measures performed in triplicate. A multiple comparison (two-way ANOVA) led to the following statistical results: **** extremely significant (P value < 0.0001), *** extremely significant (P value from 0.0001 to 0.001), ** very significant (P value from 0.001 to 0.01), * significant (P value from 0.01 to 0.05), no asterisk means not significant (P value ≥ 0.05).

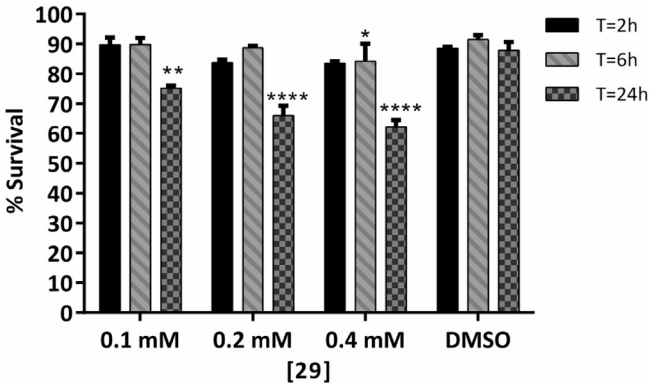

Fig. 8. Cytotoxicity on THP-1 human monocytic cell line. Percentage of cell survival as a function of time (2 h, 6 h and 24 h) and compound **29** concentration (0.1 mM - 1 × MIC, 0.2 mM - 2 × MIC and 0.4 mM - 4 × MIC) compared to the control (DMSO 1%). All values are presented as the (mean ± SD) of measures performed in triplicate. A multiple comparison (two-way ANOVA) led to the following statistical results: **** extremely significant (P value < 0.0001), *** extremely significant (P value from 0.0001 to 0.001), ** very significant (P value from 0.001 to 0.01), * significant (P value from 0.01 to 0.05), no asterisk means not significant (P value ≥ 0.05).

Table 4
Selectivity profile of compound **29**.

Enzyme or receptor	Radioligand	Control inhibitor (IC_{50}, nM)	% Inhibition
5-$HT1_A$ (h)	[^{3}H]8-OH-DPAT	[^{3}H]8-OH-DPAT (0.6)	NI
ACE (h)	–	Captopril (0.7)	66
Acetylcholinesterase (h)	–	Galanthamine (520)	NI
Arg1 (h)	–	S-(2-boronoethyl)-*l*-cysteine (13 μM)	NI
β-Lactamase (*Bacillus cereus*)	–	Clavulanic acid (11)	NI
Carbonic anhydrase II (h)	–	Acetazolamide (29)	NI
CB_1 (h)	[^{3}H]CP 55940	CP55940 (0.58)	NI
COX_1 (h)	–	Diclofenac (8)	NI
DNA Gyrase (*E. coli and S. aureus*)	–	–	NI[a]
$GABA_{A1}$ (α1,β2,γ2) (h)	[^{3}H]Muscimol	Muscimol (75)	NI
IDO (h)	–	1-L-Methyltryptophan (37 μM)	NI
Lck kinase (h)	–	Staurosporine (31)	NI
LDH (h)	–	Oxamic acid (577 μM)	NI
M_1 (h)	[^{3}H]Pirenzepine	Pirenzepine (22)	NI
MAG lipase (h)	[^{3}H]-2-OG	Disulfiram (363)	NI
MAO-A (h)	–	Clorgiline (40)	NI
PDE3A (h)	–	Milrinone (490)	NI
PHGDH (h)	–	1-(4-Chlorophenyl)-2-morpholino-2-thioxoethanone (8.7 μM)	NI
$sPLA_2$ (type V) (h)	–	Oleyloxyethyl phosphorylcholine (20 μM)	NI
Potassium Channel hERG (h)	[^{3}H]Dofetilide	Terfenadine (80)	NI
PPARα (h)	[^{3}H]WY 14643	GW7647 (52)	NI
Thrombin (h)	–	PPACK (0.103)	NI
Topo IV (*E. coli and S. aureus*)	–	–	NI[a]

[a] from Ref. [57]; NI = inhibition ≤ 30% at 10 μM; Significance criteria (Eurofins Cerep): ≥50% of inhibition.

observed that both tautomers fit very well this pocket thanks to an almost planar geometry stabilized through H-bond interactions between the thiosemicarbazide function and the 2-hydroxyphenyl moiety. This intramolecular H-bond was already mentioned in the X-ray structure of **29** (Fig. 3). In the "keto" form (Fig. 9b), the hydroxyl in the 2-position of **29** would be stabilized through H-bonding with the carbonyl oxygen of Pro311 backbone, whereas in the "enol" form (Fig. 9c), the compound would be stabilized through H-bonds between the carbonyl oxygen of Pro311 and the thiol function, and between the carbonyl oxygen of Leu94 and the enol function. Whether the "keto" or the "enol" tautomeric form is being considered, this molecular modeling analysis strongly supports the SAR reported earlier in this work, particularly regarding the key role of the hydroxyl function in the 2-position of the arylthiosemicarbazide for the proper conformation and interaction with Ddl.

4. Conclusions

This work thus allowed the identification of novel D-Ala-D-Ala ligase inhibitors with antibacterial effects on sensitive and resistant strains. This novel benzoylthiosemicarbazide series was synthesized via a straightforward procedure. Pharmacomodulations around the parent compound **3** were performed and led to interesting structure-activity relationships, particularly (i) the 2-hydroxy substituent (R_1) on the benzoylthiosemicarbazide derivatives is essential for the enzymatic inhibition, (ii) no crucial interaction is made between the right part of the thiosemicarbazide scaffold (R_2) and the enzymatic cavity and (iii) the thiosemicarbazide linker is essential for a proper recognition by Ddl.

Moreover, the antibacterial results showed that several compounds displayed promising biological activities against Gram-positive bacterial strains. Among them, the benzoylthiosemicarbazide **28** exhibited strong antibacterial potency against all tested sensitive and resistant Gram-positive species with low MIC values between 25 μM (8.91 mg/L) and 50 μM (17,81 mg/L). The ability of our compounds to prevent the growth of various bacterial strains, resistant to a wide range of currently used antibiotics, paves the way to the development of new antimicrobial agents that should be less sensitive to resistance mechanisms. A major parameter for the development of these novel drugs is lipophilicity. Indeed, an optimally balanced $logD_{7.4}$ value is needed to allow the molecules to enter bacteria and remain soluble in body fluids. The theoretical $logD_{7.4}$ for all benzoylthiosemicarbazides were calculated by mean of the ACD/Labs® program and are presented in Table 1. Our best compounds **28** and **29** against sensitive and resistant bacterial strains indeed possessed two of the highest calculated $logD_{7.4}$ among the benzoylthiosemicarbazide derivatives (X = S) of 3.40 and 3.63, respectively. In addition, the drug's ability to permeate cells was estimated by the calculation of the polar surface area (PSA). TPSA is a 2-dimensional estimation of the compound's PSA [62]. It can be observed from Table 1 that all the active molecules on bacteria showed TPSA from 105.48 to 129.27 $Å^2$, which is very encouraging given that low values (PSA < 75 $Å^2$) are usually linked to non-specific toxicity [63] and high values (PSA > 140 $Å^2$) to poor membrane permeability [64].

As emphasized in the *in vitro* evaluation, only Ddl inhibitors possessing a 2-hydroxy substituent (R_1 = 2-OH) and a thiosemicarbazide linker were able to stop bacterial growth. Furthermore, it seemed that the presence of a halogen group on the phenyl (R_2 = X-phenyl) on the right part of the molecule is beneficial to the antimicrobial activity, as observed for compounds **22**–**23**, **25**–**29**, **38** and **41**. It was also observed that electron-donating groups did not favor the antibacterial efficiency given that compounds **30**–**31**, **33** and **34** are inactive.

The model compound **29** was proved to act through a bactericidal mechanism. Moreover, a high specificity towards bacterial species compared to cytotoxicity as evaluated on THP-1 human monocytic cell line was also noticed. Indeed, 99% of bacteria are killed after 24 h of incubation at 0.1 mM (1 × the MIC value) compared to only 12% of cells.

An additional selectivity study of this compound allowed us to conclude that this 1-(2-hydroxybenzoyl)-thiosemicarbazide motif is highly selective for Ddl as only one of the twenty-three investigated systems, angiotensin converting enzyme, was slightly inhibited at 10 μM.

Finally, we demonstrated through the quantification of D-Ala, L-Ala and D-Ala-D-Ala *via* LC-MS that Ddl was effectively the *in*

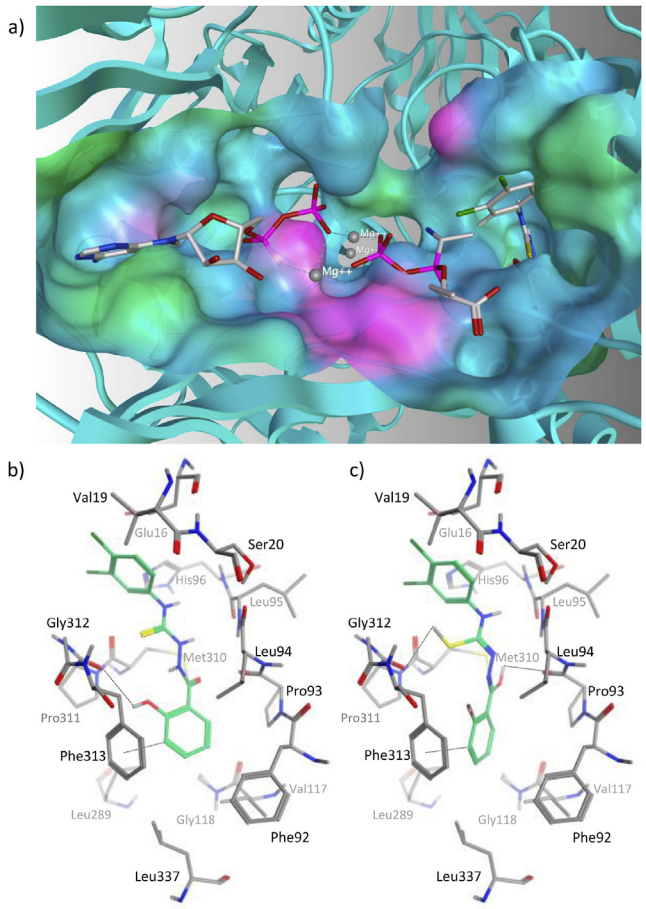

Fig. 9. Docking of the model compound **29** at the allosteric site of Ddl. **(a)** The lipophilic protein surface was built from the inhibitor-bound StaDdl crystal structure, with green and magenta representing lipophilic and hydrophilic residues, and cyan for the neutral ones. Carbon, oxygen, nitrogen, phosphorus, chlorine and hydrogens are colored in grey, red, blue, magenta, green and white respectively. Mg^{2+} ions are represented by grey spheres; ADP, methyl-phosphinophosphate, and compound **29** by sticks. **(b)** Ketone form of the model benzoylthiosemicarbazide **29**. **(c)** Enol form of the model benzoylthiosemicarbazide **29**. Carbon atoms of **29** and residues are shown in green and grey, respectively. (For interpretation of the references to color in this figure legend, the reader is referred to the Web version of this article.)

bacterio target of our benzoylthiosemicarbazides. This striking result, not only validates this series of 1-(2-hydroxybenzoyl)-thiosemicarbazides as novel antibacterial agents but also opens new perspectives for the development of novel antibiotics deprived of issues related to resistance mechanisms.

5. Experimental section

5.1. Chemistry

All reagents were purchased from chemical suppliers if commercially available and used without purification. Syntheses were performed under atmospheric pressure unless specified otherwise. Thin-layer chromatography (TLC) was performed using silica gel 60 F254 plates, with observation under UV. The ^{1}H and ^{13}C Nuclear Magnetic Resonance spectra were recorded respectively on an AVANCE II 400 MHz or 100 MHz Bruker spectrometer with $CDCl_3$ (residual internal $CHCl_3$ $\delta_H = 7.26$) or DMSO-d_6 (residual internal DMSO $\delta_H = 2.50$ ppm) as solvent. All coupling constants are measured in hertz (Hz), and the chemical shifts (δ_H and δ_C) are quoted in parts per million (ppm) relative to TMS (δ_0), which was used as the internal standard. Data are reported as follows: chemical shift, multiplicity (s = singlet, d = doublet, t = triplet, q = quartet, quint = quintet, br = broad, m = multiplet), coupling constant (Hz) and integration. Labile protons are not always visible in ^{1}H NMR spectrum. Melting points were measured on an Electrothermal IA9000 apparatus. High-resolution mass spectroscopy was carried out on an LTQ-Orbitrap XL hybrid mass spectrometer (Thermo Fisher Scientific, Bremen, Germany). Data were acquired in positive ion mode using full-scan MS with a mass range of 100–1000 *m/z*. The orbitrap operated at 30.000 resolution (FWHM definition). All experimental data were acquired using daily external calibration prior to data acquisition. Appropriate tuning of the electrospray ion source was done. The following electrospray inlet conditions were applied: flow rate, 100 μL min^{-1}; spray voltage, 5 kV; sheath gas (N_2) flow rate, 20 a.u.; auxiliary gas (N_2) flow rate, 10 a.u.; capillary temperature, 275 °C; capillary voltage, 45 V; tube lens, 80 V. High performance liquid chromatography analyses were performed on a Merck-Hitachi apparatus with quaternary pomp, automatic autosampler and UV–vis detector. The column was a Lichrospher C18 endcapped with 5 μm particles size, 250 mm long and 4.6 mm diameter. The purity of the products was determined along two methods, an isocratic system with acetonitrile/water (50:50) as mobile phase (reading at 254 nm) and the other using an elution gradient of 5–80% in acetonitrile (reading at 210 nm). The HPLC purities of the final compounds that underwent biological assessment were ≥95%.

5.1.1. General procedure for the preparation of benzohydrazides (*4*–*13*)

Various benzohydrazides **5**–**7** and **9**–**13** were obtained according to known procedures [40,65] except for benzohydrazides **4** and **8** which were commercially available. A solution of the methyl benzoate (1 equiv) in ethanol was added dropwise to 65% hydrazine monohydrate (5 equiv). The reaction mixture was then heated under reflux and stirred overnight. The reaction progress was followed up by TLC. Crude product was collected by filtration after cooling of the reaction medium and finally washed with cold ethanol unless specified otherwise. The desired benzohydrazides were used without any further purification.

The analysis of spectral data (^{1}H and ^{13}C NMR), the yields, HRMS, Mp and R_f of these precursors are presented in Supplementary Information.

5.1.2. General procedure for the preparation of thiosemicarbazides (*3*, *14*–*48* and *51*–*52*)

A series of thiosemicarbazides **3**, **14**–**48** and **51**–**52** were prepared according to a procedure adapted from the literature [40,41] by adding an isothiocyanate (1 equiv) dropwise to a solution of benzohydrazide (1 equiv) in methanol. The reaction mixture was stirred at room temperature and its progress was followed by TLC. The precipitate was then collected by filtration, washed with cold ethanol and then recrystallized from ethanol as many times as necessary to obtain a pure product.

Target compounds are presented below, the analysis of spectral data (^{1}H and ^{13}C NMR), the yields, HRMS, Mp and R_f of other compounds are however presented in Supplementary Information.

*1-(2-Hydroxybenzoyl)-4-phenyl-3-thiosemicarbazide (**3**).* [66] This compound was synthesized according to the general procedure described above using synthesized 2-hydroxybenzohydrazide **5** (0.29 g, 1.93 mmol) and phenyl isothiocyanate (0.26 g, 1.93 mmol) in methanol (20 mL). After 7 h of reaction, the pure product was collected as a white powder (0.16 g, 28%). R_f 0.75 (PE/EtOAc 4:6). Mp: 187.8–190.0 °C. ^{1}H NMR (400 MHz, DMSO-d_6): δ_H (ppm) 6.92–7.01 (m, 2H, Ar), 7.17 (dd, $J = 7.4$ Hz, 1H, ArH), 7.37 (dd, $J = 7.8$ Hz, 2H, ArH), 7.44–7.56 (m, 3H, Ar), 7.91 (d, $J = 5.6$ Hz, 1H,

Ar), 9.7–10.5 (m, 1.7H and 0.3H, NH), 10.6–11.5 (brs, 0.7H and 0.3H, NH), 11.91 (s, 1H, OH). ^{13}C NMR (100 MHz, DMSO-d_6): δ_C (ppm) 115.13 (Ar), 117.12 (Ar), 118.87 (Ar), 125.07 (Ar), 125.79 (Ar), 128.09 (Ar), 128.81 (Ar), 134.01 (Ar), 139.07 (Ar), 159.39 (Ar), 168.94 (C=O), 180.85 (C=S). HRMS (ESI$^+$): *m/z* calcd for $C_{14}H_{14}N_3O_2S$ $(M + H)^+$ 288.08012, found 288.08008.

*1-Benzoyl-4-phenyl-3-thiosemicarbazide (**14**)* [67]. This compound was synthesized according to the general procedure described above using commercial benzohydrazide **4** (0.54 g, 4 mmol) and phenyl isothiocyanate (0.54 g, 4 mmol) in methanol (20 mL). After 17 h of reaction, the pure product was collected as white needles (0.82 g, 76%). R_f 0.3 (PE/EtOAc 5:5). Mp: 162.6–163.1 °C. ^{1}H NMR (400 MHz, DMSO-d_6): δ_H (ppm) 7.17 (dd, $J = 7.3$ Hz, 1H, ArH), 7.34 (dd, $J = 7.7$ Hz, 2H, ArH), 7.45 (m, 2H, ArH), 7.51 (dd, $J = 7.5$ Hz, 2H, ArH), 7.59 (dd, $J = 7.3$ Hz, 1H, ArH), 7.97 (d, $J = 7.4$ Hz, 2H, ArH), 9.73 (s, 1H, NH), 9.83 (brs, 1H, NH), 10.56 (s, 1H, NH). ^{13}C NMR (100 MHz, DMSO- d_6): δ_C (ppm) 125.22 (Ar), 125.80 (Ar), 128.03 (Ar), 128.29 (Ar), 131.91 (Ar), 132.56 (Ar), 139.06 (Ar), 165.95 (C=O), 181.05 (C=S). HRMS (ESI$^+$): *m/z* calcd for $C_{14}H_{14}N_3OS$ $(M + H)^+$ 272.08521, found 272.08499.

*4-(3,4-Dichlorophenyl)-1-(2-hydroxybenzoyl)-3-thiosemicarbazide (**29**)* [68]. This compound was synthesized according to the general procedure described above using synthesized 2-hydroxybenzohydrazide **5** (0.43 g, 2.55 mmol) and 3,4-dichlorophenyl isothiocyanate (0.52 g, 2.55 mmol) in methanol (10 mL). After 24 h of reaction, the pure product was collected as white needles (0.56 g, 63%). R_f 0.19 (PE/EtOAc 4:6). Mp: 200.0–201.0 °C. ^{1}H NMR (400 MHz, DMSO-d_6): δ_H (ppm) 6.91–7.02 (m, 2H, ArH), 7.47 (ddd, $J = 7.6$ Hz, $J = 0.8$ Hz, 1H, ArH), 7.54 (dd, $J = 8.8$ Hz, $J = 2.1$ Hz, 1H, ArH), 7.60 (d, $J = 9.2$ Hz 1H, ArH), 7.80–7.96 (m, 2H, ArH), 9.90–10.30 (m, 2H, NH), 10.5–11.5 (brs, 1H, NH), 11.88 (s, 1H, OH). ^{13}C NMR (100 MHz, DMSO-d_6): δ_C (ppm) 120.13 (Ar), 122.46 (Ar), 124.14 (Ar), 128.90 (Ar), 130.74 (Ar), 132.03 (Ar), 134.02 (Ar), 135.05 (Ar), 135.32 (Ar), 139.45 (Ar), 144.55 (Ar), 164.73 (Ar), 174.01 (C=O), 186.05 (C=S). HRMS (ESI$^+$): *m/z* calcd for $C_{14}H_{12}Cl_2N_3O_2S$ $(M + H)^+$ 356.00218, found 356.00235.

5.1.3. General procedure for the preparation of semicarbazides (**53**–**54**) [44]

The semicarbazides **53** and **54** were prepared by adding an isocyanate (1 equiv) to a benzohydrazide (1 equiv) in methanol. The reaction mixture was stirred under reflux and its progress was followed up by TLC. The precipitate was then collected by filtration and washed with cold methanol.

*2-Benzoyl-N-(3,4-dichlorophenyl)hydrazine-1-carboxamide (**53**)* [69]. This compound was synthesized according to the general procedure described above using commercial benzohydrazide **4** (0.37 g, 2.72 mmol) and 3,4-dichlorophenyl isocyanate (0.51 g, 2.72 mmol) in methanol (20 mL). After 17 h of reaction, the pure product was collected as white needles (0.28 g, 32%). R_f 0.54 (PE/EtOAc 5:5). Mp: 214.5–215.0 °C. ^{1}H NMR (400 MHz, DMSO-d_6): δ_H (ppm) 7.36–7.54 (m, 4H, ArH), 7.58 (ddd, $J = 7.3$ Hz, $J = 2.2$ Hz, 1H, ArH), 7.87 (d, $J = 2.2$ Hz, 1H, ArH), 7.91 (d, $J = 7.3$ Hz, 2H, ArH), 8.44 (brs, 1H, NH), 9.18 (brs, 1H, NH), 10.31 (s, 1, NH). ^{13}C NMR (100 MHz, DMSO-d_6): δ_C (ppm) 118.66 (Ar), 119.68 (Ar), 123.14 (Ar), 127.56 (Ar), 128.38 (Ar), 130.44 (Ar), 130.80 (Ar), 131.83 (Ar), 132.46 (Ar), 140.02 (Ar), 159.94 (C=O), 166.43 (C=O). HRMS (ESI$^+$): *m/z* calcd for $C_{14}H_{12}Cl_2N_3O_2$ $(M + H)^+$ 324.03011, found 324.03021.

*N-(3,4-dichlorophenyl)-2-(2-hydroxybenzoyl)hydrazine-1-carboxamide (**54**).* This compound was synthesized according to the general procedure described above using synthesized 2-hydroxybenzohydrazide **5** (0.40 g, 2.65 mmol) and 3,4-dichlorophenyl isocyanate (0.50 g, 2.67 mmol) in methanol (20 mL). After 17 h of reaction, pure product was collected as white powder (0.34 g, 37%). R_f 0.74 (PE/EtOAc 5:5). Mp: 254.0–256.0 °C. ^{1}H NMR (400 MHz, DMSO-d_6): δ_H (ppm) 6.89–6.99 (m, 2H, ArH), 7.38–7.47 (m, 2H, ArH), 7.51 (d, $J = 8.8$ Hz, 1H, ArH), 7.87 (d, $J = 2.3$ Hz, 1H, ArH), 7.89 (dd, $J = 7.9$ Hz, $J = 1.5$ Hz, 1H), 8.59 (s, 1H, NH), 9.24 (brs, 1H, NH), 10.45 (brs, 1H, NH), 11.92 (brs, 1H, OH). ^{13}C NMR (100 MHz, DMSO-d_6): δ_C (ppm) 114.65 (Ar), 117.29 (Ar), 118.67 (Ar), 118.92 (Ar), 119.68 (Ar), 123.28 (Ar), 128.36 (Ar), 130.47 (Ar), 130.85 (Ar), 134.11 (Ar), 139.87 (Ar), 155.17 (Ar), 159.30 (C=O), 168.60 (C=O). HRMS (ESI$^+$): *m/z* calcd for $C_{14}H_{12}Cl_2N_3O_3$ $(M + H)^+$ 340.02502, found 340.02505.

5.1.4. X-ray crystal structure determination of compound **29**

A single crystal of compound **29** was obtained by slow evaporation from a solution of MeOH/DMSO. Data were then collected at room temperature on a Gemini diffractometer (Oxford Diffraction Ltd) equipped with a Ruby CCD detector using Enhance (Cu) X-ray Source. Data collection program: CrysAlis CCD (Oxford Diffraction Ltd), data reduction: CrysAlis RED (Oxford Diffraction Ltd), structure solution: SHELXS, structure refinement (on *F* [2]): SHELXL-97 [70], data analysis: PLATON [71]. A multi-scan procedure was applied to correct for absorption effects. Hydrogen atom positions were calculated and refined isotropically using a riding model. Crystal size $0.04 \times 0.06 \times 0.60$ mm; monoclinic, $P2_1/c$, $a = 10.9037(2)$, $b = 6.7368(1)$, $c = 26.5219(6)$ Å, $\beta = 96.558(2)°$, $V = 1935.45(6)$ Å^3, $Z = 4$, $\rho_{calc} = 1.491$ g cm^{-3}, $F_{000} = 896$, λ Cu Kα = 1.54184 Å, $\theta_{max} = 66.6°$, 10601 total measured reflections, 3391 independent reflections ($R_{int} = 0.034$), 3056 observed reflections ($I > 2\,\sigma(I)$), $\mu = 5.229$ mm^{-1}, 253 parameters, R_1 (observed data) = 0.0434, R_1 (all data) = 0.1242, S = GooF = 1.06, Δ/s.u. = 0.000, residual $\rho_{max} = 0.40$ e Å^{-3}, $\rho_{min} = -0.41$ e Å^{-3}.

5.2. Biology

All the graphs were obtained with *GraphPad Prism 6* software (San Diego, CA). The reagents used for the enzymatic assay (BIOMOL® Green reagent, phosphate standard 800 μM) were purchased from Enzo Life Sciences, Inc (Farmingdale, NY). The UV spectra were recorded at room temperature on a Spectramax® M2E spectrophotometer (Molecular Devices, LLC, Sunnyvale, CA) in 96-well plates. The enzyme used was *Enterococcus faecalis* polyHis-DdlB produced and purified by our care. *E. faecalis* BM 4390, *E. faecalis* JH2-2::C1 and *E. faecalis* BM 4575 were received from Prof Patrice Courvalin, Institut Pasteur, Paris, France. *S. aureus* MU 50, VRS-1 and *S. aureus* NRS 119 were obtained from the NARSA (Network on Antimicrobial Resistance in Staphylococcus Aureus), BEI Resources, Manassas, VA. *S. aureus* SA 325 and *S. aureus* SA 481 were received from Prof. Peter Appelbaum, Hershey Medical Center, Hershey, PA. D-Ala, L-Ala and Marfey's reagent (1-fluoro-2,4-dinitripheny-L-5-alanine amide) were purchased from TCI Europe N.V. (Zwijndrecht, Belgium) and D-Ala-D-Ala from Fluorochem Ltd (Derbyshire, UK). Solvent used in LC-MS runs had the quality required for such analyses. LC–MS/MS was performed on a UHPLC system (Acquity H-Class, Waters) coupled to a tandem-quadrupole mass spectrometer (Xevo TQ-S, Waters). All chromatographic separations were achieved on an Acquity UPLC® BEH C18 column (1.7 μm, 2.1 mm × 50 mm, Waters, Milford, Massachusetts) equipped with an inline filter. All centrifuge operations were performed on an Eppendorf 5810R refrigerated centrifuge.

5.2.1. Production and purification of the recombinant His-tagged DdlB

5.2.1.1. Construction of expression vector for Enterococcus faecalis Ddl. *Enterococcus faecalis* JH2-2 total DNA [72] was extracted as described [73]. The *ddl* gene was amplified by PCR using the Phusion® High-Fidelity DNA Polymerase (New England Biolabs, Ipswich, MA) and a pair of primers including a NcoI (5′-

GAGGAATTAACCATGGCTAAGATTATTTTGTTG-3′) and an PstI (5′–CCCATATGGTACCAGCTGCAGTTTAAAACGATTCAAAGCTAACTG-3′) restriction sites (underlined). The *ddl* gene was cloned into the expression pBAD/Myc-His-A vector (Invitrogen) under the control of the L-arabinose inducible promoter [74] between the NcoI and PstI restriction sites. The sequence of the PCR fragment was completely checked on both strains using the pBAD forward and reverse sequencing primers. The resulting plasmid encoding a protein with a C-terminal 6-His tag served to transform the *E. coli* LMG194 expression strain (Invitrogen [75]).

5.2.1.2. Overproduction of the Ddl-His$_6$ enzyme. The production and purification of Ddl-His$_6$ enzyme were performed according to previous work from our group [33]. Transformed bacteria *E. coli* LMG194 containing the pBAD/Ddl-*Myc*-His plasmid were inoculated by adding 1/50 of preculture (performed overnight) in minimal medium (RM media, Invitrogen [76]) containing 0.2% glucose and 100 mg/L ampicillin. This culture was placed in the incubator and grown at 37 °C until an optical density (OD) at 600 nm of 0.4. At this point, L-arabinose was added to the culture to reach 2% of the final concentration and the latter was placed for overnight growth at 20 °C under shaking. All subsequent steps were performed at 4 °C. Bacteria were then harvested by centrifugation, resuspended in a 30-fold smaller volume of buffer A (50 mM Hepes pH 8.0, 5 mM $MgCl_2.6H_2O$, 10 mM imidazole (U.V. = 0) and 10% glycerol). Phenylmethylsulfonyl fluoride (PMSF) 100 mM, a serine protease inhibitor, was added to the bacterial suspension (100 × dilution) as well as benzonase (10.000 × dilution). Lyse was performed by 3 successive passages in a French Press operating at 1000–1500 psi (SLM Aminoco). Cellular debris, or insoluble fraction, were removed by centrifugation (30 min, 18 000 g). The supernatant, or soluble fraction, was then filtered through a 0.45 μm filter and contained the desired protein.

5.2.1.3. Purification of the Ddl-His$_6$ enzyme. 30 mL of supernatant were injected on the Ni-NTA column (HisTrap GE Healthcare) previously washed with cold buffer A (50 mM Hepes pH 8.0, 5 mM $MgCl_2.6H_2O$, 10 mM imidazole (U.V. = 0) and 10% glycerol). Proteins having low natural affinity for Ni were eluted by 20 mL of 10% buffer B (50 mM Hepes pH 8.0, 5 mM $MgCl_2.6H_2O$, 500 mM imidazole (U.V. = 0), 300 mM NaCl and 10% glycerol), then His-tagged protein was recovered thanks to an elution gradient of buffer B (50 mL, 10%–100%). Eluate was dialyzed overnight against a 142.8-fold higher volume of buffer C (50 mM Hepes pH 7.2, 150 mM KCl, 5 mM $MgCl_2.6H_2O$, 5 mM glutathione reduced form (GSH) and 20% glycerol) at 4 °C. The His-tagged protein purity was checked by SDS-polyacrylamide gel electrophoresis (Novex Tris-Glycine Gels 14%, Invitrogen [77]): a single band at 42 kDa was observed after Coomassie Blue staining. The purified protein concentration was measured by the method of Bradford using bovine serum albumin as standard (Pierce™ BCA Protein Assay Kit, ThermoFisher Scientific) and determined to be 2.04 mg/mL. Pure fractions were stored in buffer C at −80 °C.

5.2.2. Inhibition of the Ddl-His$_6$ enzyme

The activity of DdlB was monitored with the colorimetric malachite green method in which orthophosphate generated during the reaction is measured, performed exactly as described in the literature [45].

5.2.2.1. Screening of the compounds. Each compound was tested at a concentration of 10 μM for its ability to inhibit DdlB activity. Assays were performed with a pre-incubation of 30 min at 30 °C between the enzyme, the inhibitor and the ATP. Then, the substrate was added and incubated with the mixture for 20 min at 30 °C. The composition of this mixture (final volume: 50 μL) was 20 mM Tris.HCl (pH 7.4), 10 mM $MgCl_2$, 10 mM KCl, 10 μM inhibitor, 500 μM ATP, 1 mM of D-Ala and 20 mg/L of purified DdlB. All compounds were soluble in the assay mixture containing 10% DMSO. After the incubation, 100 μL of Biomol® Green reagent containing 10% DMSO were added and the absorbance was read at 650 nm after 25 min.

5.2.2.2. Determination of the IC$_{50}$. For compounds showing significant inhibitory activity at 10 μM (>70%) with respect to a similar assay without the inhibitor, IC_{50} values were determined under similar conditions to the screening. Each compound was tested at 7 concentrations (10^{-8}, 10^{-7}, 3.10^{-7}, 10^{-6}, 3.10^{-6}, 10^{-5} and 3.10^{-5} or 5.10^{-5} M). The absorbance was read at 650 nm after 25 min of reaction with the Biomol® Green reagent, 10 min of incubation with the substrate and a preincubation with the inhibitor, the enzyme and ATP of 30 min at 30 °C. Additionally, we performed several IC_{50} by varying incubation time with our hit compound. Inhibitor **3** was preincubated with the enzyme for 10, 30, 60, 90 and 120 min before the reaction was initiated as described above (the same final concentrations were those described for IC_{50}).

5.2.2.3. Rapid dilution assay. The reversibility of the enzymatic inhibition by benzoylthiosemicarbazide **29** was evaluated by the rapid dilution method. Three conditions were tested with similar assay composition to those used for the screening: a positive control medium without inhibitor (20 mg/L of Ddl), a medium with 3 μM of **29** and 200 mg/L of the enzyme, and a negative control with 3 μM of **29** and 20 mg/L of the enzyme. After a preincubation of 30 min at 30 °C between the enzyme, the inhibitor **29** and the ATP, the concentrated medium was diluted 10 times to mimic the composition of the control with 3 μM of **29** and 20 mg/L of the enzyme. The absorbance was then read after 20 min of incubation with the substrate at 30 °C and the addition of Biomol® Green reagent.

5.2.2.4. Competition with D-Ala. Kinetics for D-Ala were performed with compound **29** at 3 concentrations (0 μM, 1 μM and 10 μM) and increasing concentrations in substrate (0.75, 1, 3, 5, 10, 15, 20 and 50 mM) and 500 μM of ATP. The operating conditions were similar to the ones previously described. Before the quenching by Biomol® Green reagent, the wells containing 3, 5, 10, 15, 20 and 50 mM of D-Ala were diluted 10 times with respect to the linearity zone.

5.2.2.5. Competition with ATP. Kinetics for ATP were performed with compound **29** at 3 concentrations (0 μM, 1 μM and 10 μM), increasing concentrations in cofactor (10, 20, 30, 50, 100, 500 and 1000 μM) and 50 mM of D-Ala. The operating conditions were similar to the ones previously described except for the D-Ala concentration. Before the quenching by Biomol Green reagent, the wells containing 30, 50, 100, 500 and 1000 μM of ATP were diluted 10 times to respect the linearity zone.

5.2.2.6. Selectivity assays. The inhibitory activities of **29** were assessed according to the literature for the following enzymes: Arginase 1 (Arg1) [78], indoleamine 2,3-dioxygenase (IDO) [79], lactate dehydrogenase (LDH) [80], monoacylglycerol lipase (MAGL) [81], and phosphoglycerate dehydrogenase (PHGDH) [82]. Other enzymes and receptors binding assays were performed at Eurofins Cerep (France). Their criteria for significance is ≥ 50% inhibition.

5.2.3. Microbiological evaluation

5.2.3.1. Antimicrobial activity. MICs were determined by microdilution method in cation-adjusted Muller-Hinton broth (CAMHB) (Becton-Dickinson, NJ, USA), following the recommendations of the US Clinical and Laboratory Standards Institute (CLSI) [84], using an

initial inoculum of 10^6 bacteria/mL, with a final concentration of 1% DMSO (this concentration was proved not to impair bacterial growth). The potential antimicrobial agents were prepared in a two-fold dilution series in CAMHB with 2% DMSO (Sigma-Aldrich), and then diluted with the same volume of bacterial suspension. Microwell plates with 96 wells were then incubated for 18–24 h at 37 °C. The MIC was taken as the lowest concentration of potential antimicrobial agent that prevented the visible growth of bacteria [29,33].

5.2.3.2. Time-kill studies. Time-kill curves were performed according to CLSI method [85]. *S. aureus* ATCC 25923 was grown overnight at 37 °C in CAMHB under shaking. The bacterial suspension was then centrifuged for 7 min at 4000 rpm and the supernatant recollected. Cells were diluted in medium to obtain 2.10^6 CFU/mL. Compound **29** in DMSO, adjusted to a concentration of 1, 2 or 5 times the MIC, was then added to obtain a starting inoculum of 10^6 CFU/mL with 5% DMSO (5% DMSO alone was tested in parallel). The positive control contained only 10^6 CFU/mL. Aliquots (20 μL) of the cultures were removed at 0 h, 1 h, 2 h, 5 h, 7 h and 24 h of incubation. A series of 10-fold dilutions were prepared in phosphate buffer saline (PBS) and plated on tryptic soy agar (TSA). The number of viable cells on TSA was determined after 24 h of incubation at 37 °C. The rate of killing was determined by calculating the reduction of viable bacteria ($\log_{10}$ CFU/mL) at different sampling times for all the inhibitor concentrations. Bactericidal activity is defined as a $\geq$3-$\log_{10}$ reduction of the initial CFU amount in 24 h.

5.2.3.3. LC-MS/MS analysis of L-Ala, D-Ala and D-Ala-D-Ala levels in bacterio. Preparation of bacterial extracts. The bacterial sample was prepared according to the literature for *S. aureus* strains [60]. *S. aureus* ATCC 25923 (2 × 25 mL) was grown overnight at 37 °C in MHB 5% DMSO under shaking. The bacterial suspension was then centrifuged for 7 min at 4000 rpm and the cells pellet was resuspended in 20 mL of MHB 5% DMSO. The appropriate volume of this solution was added to 200 mL of MHB 5% DMSO to obtain an absorbance of 0.05 at 600 nm (OD_{600}) and the culture was subsequently incubated at 37 °C under shaking at 300 rpm until the OD_{600} reached 0.6. Compound **29** was then added to 60 mL-portions of this culture to a final concentration of 2 × MIC (0.2 mM) so that the incubation time ranges from 0, 5, 10, 20–30 min. Control cultures were grown without antibiotic or with 2 × MIC of DCS (0.63 mM). After the incubation time, all flask were cooled in an ice/water bath and three 10 mL-aliquots of each were poured into cold centrifugation tubes. Bacteria were then pelleted at 4000 rpm for 10 min at 4 °C and cell pellets washed with 400 μL of M9 minimal medium (Na_2HPO_4 30 g/L, KH_2PO_4 15 g/L, NH_4Cl 5 g/L and NaCl 2.5 g/L). These centrifugation/washing steps were repeated 3 times. After the third wash, cell pellets were resuspended in 100 μL of M9 minimal medium and 400 μL of ice-cold lysis solvent (MeOH/H_2O/formic acid, 80:20:0.1 v/v) were then added. After 5–10 min on ice by vortexing occasionally, the lysed bacteria were centrifuged at 4000 rpm for 10 min at 4 °C. Supernatants (~500 μL) were then harvested and keept on ice for the subsequent derivatization of 45 μL-samples of each triplicate.

Derivatization with Marfey's reagent and optimization in LC, MS and MS/MS. The optimization of the LC-MS/MS method and the derivatization procedure were carried out according to the literature [59]. First, L-Ala, D-Ala and D-Ala-D-Ala metabolites purchased from commercial source were derivatized with Marfey's reagent either alone or as a mixture to optimize the separation and the MS and MS/MS parameters. Calibration curves were performed with dilutions of these samples in water or bacterial extracts from 15 to 0 μM. All the derivatization and the following steps were carried out under dark condition (absence of light) [83]. These mixtures were then desalted on a C18 SPE column prior to MS and MS/MS optimization. The optimized MS parameters are described hereunder. The MS/MS detection was done with electrospray ionization (ESI) in the positive mode and multiple reaction monitoring (MRM). The capillary voltage was set to 3.0 kV, the source offset was 50 V, the cone gas flow was 150 L/h, the source block temperature was 150 °C and the nitrogen desolvation gas was heated to 500 °C with a flow rate of 1000 L/h. Four transitions were followed: two corresponding to the neutral loss of 45 Da-Marfey's terminal protonated amide [M + H-45]+) for the quantification: 342.20 > 297.20 with cone voltage at 25.0 V and collision energy at 15.0 ev (D-Ala and L-Ala, quantitative ion product); 413.25 > 368.20 with cone voltage at 25.0 V and collision energy at 15.0 ev (D-Ala-D-Ala, quantitative ion product) and two transitions for the qualification: 342.20 > 205.35 with cone voltage at 25.0 V and collision energy at 30.0 ev (D-Ala and L-Ala, qualitative ion product); 413.25 > 251.25 with cone voltage at 25.0 V and collision energy at 25.0 ev (D-Ala-D-Ala, qualitative ion product). The dwell time was set to 0.034 s. The tandem mass spectrometer was operated with MassLynx/Target Lynx Software version 4.1 (Waters). Finally, the chromatographic conditions were set as followed: the elution was performed at 0.5 mL/min at a temperature of 40 °C with a starting gradient of 90% solvent A (0.1% formic acid in water) and 10% solvent B (acetonitrile). After 1 min, the gradient linearly ramped to 64.5% solvent A and 35.5% solvent B until 8 min. The proportion of B was then return to 10% and reequilibration was done during 2 min before the next injection. UHPLC-MS/MS analysis was performed with an injection volume of 2 μL for each derivatized sample.

5.2.3.4. Determination of toxicity for mammalian cells. Cell viability was determined on human THP-1 cells by use of the Trypan blue exclusion assay [86]. Human myelomonocytic THP-1 cells (ATCC TIB-202) [87] were cultivated in RPMI-1640 medium supplemented with 10% fetal calf serum (Gibco/Life Technologies Corporation (Paisley, UK)) as described previously [88]. Compound **29** was added to cell suspension to obtain final concentrations of 10^{-4} M, 2.10^{-4} M and 4.10^{-4} M at 1% DMSO (1, 2 and 5 times the MIC for *S. aureus* ATCC 25923). The medium was incubated at 37 °C in a 5% CO_2 atmosphere and aliquots (50 μL) were removed at 2 h, 4 h and 24 h. Trypan blue solution 0.4% (Gibco/Life Technologies Corporation (Paisley, UK)) was then added in a 1:1 (v:v) proportion to the cell suspension. After 5 min of incubation with the dye, the percentage of dead cells was calculated as the number of cells stained in blue *vs* the total number of cells as counted using optical microscopy.

Author contributions

Conceived and designed the experiments: AA, LT, RF, FVB. Protein production and purification: AA, BJ, SL. Compounds synthesis and characterization: AA, LT. Enzymatic assays: AA, LT. Biological activities: AA. UHPLC-MS/MS experiments: AA, LP. Crystal growth and X-ray structure determination: AA, JW. Manuscript preparation: AA, RF, FVB. All authors have given approval to the final version of the manuscript.

Competing interest

The authors declare no competing financial interest.

Acknowledgment

We are grateful to B. Es Saadi, E. Yildiz, P. Simon, Dr. O. Verlaine, K.Santos and V. Yfantis for expert technical assistance and to Dr. S.

Ravez for helpful discussions. Dr. M.–F. Hérent and Prof. G. Muccioli (UCL, BPBL) are gratefully acknowledged for assistance with HRMS. LT is a research fellow (grant number 28252262) and FVB is research director from the Fonds de la Recherche Scientifique–FNRS, Belgium. This work was supported by the Université Catholique de Louvain, Belgium. Prof. P. Courvalin (Institut Pasteur, Paris, France) kindly provided *Enterococcus* strains.

Appendix A. Supplementary data

Supplementary data to this article can be found online at https://doi.org/10.1016/j.ejmech.2018.09.067.

Abbreviations

CAMHB	cation-adjusted Muller-Hinton broth
CA-MRSA	community-acquired MRSA
CFU	colony-forming unit
CIP	ciprofloxacin
DCS	D-cycloserine
Ddl	D-alanine-D-alanine ligase
DD-ligases	D-Ala-D-Ala, D-Ala-D-Lac and D-Ala-D-Ser ligases
GlcNAc	N-acetylglucosamine
HA-MRSA	hospital-acquired MRSA
LZD	linezolid
MurNAc	N-acetylmuramic acid
Ph	Phenyl
PE	petroleum ether
S	solubility
StaDDl	*S. aureus* Ddl
TPSA	topological polar surface area
TSA	tryptic soy agar
VAN	vancomycin
VISA	vancomycin intermediate resistant *S. aureus*
VRSA	vancomycin resistant *S. aureus*.

References

[1] Antimicrobial Resistance: Global Report on Surveillance, Wolrd Health Organization, 2014.
[2] L.L. Silver, Does the cell wall of bacteria remain a viable source of targets for novel antibiotics? Biochem. Pharmacol. 71 (7) (2006) 996–1005.
[3] A.L. Lovering, S.S. Safadi, N.C. Strynadka, Structural perspective of peptidoglycan biosynthesis and assembly, Annu. Rev. Biochem. 81 (2012) 451–478.
[4] B.G. Spratt, Resistance to antibiotics mediated by target alterations, Science 264 (5157) (1994) 388–393.
[5] G.D. Wright, C.T. Walsh, D-Alanyl-D-alanine ligases and the molecular mechanism of vancomycin resistance, Acc. Chem. Res. 25 (10) (1992) 468–473.
[6] I. Tytgat, E. Colacino, P.M. Tulkens, J.H. Poupaert, M. Prevost, F. Van Bambeke, DD-ligases as a potential target for antibiotics: past, present and future, Curr. Med. Chem. 16 (20) (2009) 2566–2580.
[7] L.E. Zawadzke, T.D. Bugg, C.T. Walsh, Existence of two D-alanine:D-alanine ligases in Escherichia coli: cloning and sequencing of the ddlA gene and purification and characterization of the DdlA and DdlB enzymes, Biochemistry 30 (6) (1991) 1673–1682.
[8] M. Arthur, P. Reynolds, P. Courvalin, Glycopeptide resistance in enterococci, Trends Microbiol. 4 (10) (1996) 401–407.
[9] C. Fan, P.C. Moews, C.T. Walsh, J.R. Knox, Vancomycin resistance: structure of D-alanine:D-alanine ligase at 2.3 a resolution, Science 266 (5184) (1994) 439–443.
[10] C. Fan, I.S. Park, C.T. Walsh, J.R. Knox, D-alanine:D-alanine ligase: phosphonate and phosphinate intermediates with wild type and the Y216F mutant, Biochemistry 36 (9) (1997) 2531–2538.
[11] J.H. Lee, Y. Na, H.E. Song, D. Kim, B.H. Park, S.H. Rho, Y.J. Im, M.K. Kim, G.B. Kang, D.S. Lee, S.H. Eom, Crystal structure of the apo form of D-alanine: D-alanine ligase (Ddl) from Thermus caldophilus: a basis for the substrate-induced conformational changes, Proteins 64 (4) (2006) 1078–1082.
[12] S. Liu, J.S. Chang, J.T. Herberg, M.M. Horng, P.K. Tomich, A.H. Lin, K.R. Marotti, Allosteric inhibition of Staphylococcus aureus D-alanine:D-alanine ligase revealed by crystallographic studies, Proc. Natl. Acad. Sci. U.S.A. 103 (41) (2006) 15178–15183.
[13] F.C. Neuhaus, W.P. Hammes, Inhibition of cell wall biosynthesis by analogues and alanine, Pharmacol. Ther. 14 (3) (1981) 265–319.
[14] Y. Vo-Quang, D. Carniato, L. Vo-Quang, A.M. Lacoste, E. Neuzil, F. Le Goffic, (1-Amino-2-propenyl) phosphonic acid, an inhibitor of alanine racemase and D-alanine:D-alanine ligase, J. Med. Chem. 29 (4) (1986) 579–581.
[15] K. Duncan, C.T. Walsh, ATP-dependent inactivation and slow binding inhibition of Salmonella typhimurium D-alanine:D-alanine ligase (ADP) by (aminoalkyl)phosphinate and aminophosphonate analogues of D-alanine, Biochemistry 27 (10) (1988) 3709–3714.
[16] K. Duncan, W.S. Faraci, D.S. Matteson, C.T. Walsh, (1-Aminoethyl)boronic acid: a novel inhibitor for Bacillus stearothermophilus alanine racemase and Salmonella typhimurium D-alanine:D-alanine ligase (ADP-forming), Biochemistry 28 (8) (1989) 3541–3549.
[17] S. Putty, A. Rai, D. Jamindar, P. Pagano, C.L. Quinn, T. Mima, H.P. Schweizer, W.G. Gutheil, Characterization of d-boroAla as a novel broad-spectrum antibacterial agent targeting d-Ala-d-Ala ligase, Chem. Biol. Drug Des. 78 (5) (2011) 757–763.
[18] F.C. Neuhaus, J.L. Lynch, The enzymatic synthesis of D-alanyl-D-alanine. 3. On the inhibition of D-alanyl-D-alanine synthetase by the antibiotic D-cycloserine, Biochemistry 3 (1964) 471–480.
[19] G.A. Prosser, L.P. de Carvalho, Kinetic mechanism and inhibition of Mycobacterium tuberculosis D-alanine:D-alanine ligase by the antibiotic D-cycloserine, FEBS J. 280 (4) (2013) 1150–1166.
[20] G.A. Prosser, L.P. de Carvalho, Reinterpreting the mechanism of inhibition of Mycobacterium tuberculosis D-alanine:D-alanine ligase by D-cycloserine, Biochemistry 52 (2013) 7145–7149.
[21] S. Halouska, R.J. Fenton, D.K. Zinniel, D.D. Marshall, R.G. Barletta, R. Powers, Metabolomics analysis identifies d-Alanine-d-Alanine ligase as the primary lethal target of d-cycloserine in mycobacteria, J. Proteome Res. 13 (2) (2013) 1065–1076.
[22] W.W. Yew, C.F. Wong, P.C. Wong, J. Lee, C.H. Chau, Adverse neurological reactions in patients with multidrug-resistant pulmonary tuberculosis after coadministration of cycloserine and ofloxacin, Clin. Infect. Dis. 17 (2) (1993) 288–289.
[23] S. David, Synergic activity of D-cycloserine and beta-chloro-D-alanine against Mycobacterium tuberculosis, J. Antimicrob. Chemother. 47 (2) (2001) 203–206.
[24] W.H. Parsons, A.A. Patchett, H.G. Bull, W.R. Schoen, D. Taub, J. Davidson, P.L. Combs, J.P. Springer, H. Gadebusch, B. Weissberger, et al., Phosphinic acid inhibitors of D-alanyl-D-alanine ligase, J. Med. Chem. 31 (9) (1988) 1772–1778.
[25] P.K. Chakravarty, W.J. Greenlee, W.H. Parsons, A.A. Patchett, P. Combs, A. Roth, R.D. Busch, T.N. Mellin, (3-Amino-2-oxoalkyl)phosphonic acids and their analogues as novel inhibitors of D-alanine:D-alanine ligase, J. Med. Chem. 32 (8) (1989) 1886–1890.
[26] F.C. Neuhaus, The enzymatic synthesis of D-alanyl-D-alanine. II. Kinetic studies on D-alanyl-D-alanine synthetase, J. Biol. Chem. 237 (1962) 3128–3135.
[27] G.E. Besong, J.M. Bostock, W. Stubbings, I. Chopra, D.I. Roper, A.J. Lloyd, C.W.G. Fishwick, A.P. Johnson, A de novo designed inhibitor of d-Ala–d-Ala ligase from E. coli, Angew. Chem. Int. Ed. 44 (2005) 6403–6406.
[28] A. Kovač, V. Majce, R. Lenaršič, S. Bombek, J.M. Bostock, I. Chopra, S. Polanc, S. Gobec, Diazenedicarboxamides as inhibitors of d-alanine-d-alanine ligase (Ddl), Bioorg. Med. Chem. Lett 17 (7) (2007) 2047–2054.
[29] A. Kovac, J. Konc, B. Vehar, J.M. Bostock, I. Chopra, D. Janezic, S. Gobec, Discovery of new inhibitors of D-alanine:D-alanine ligase by structure-based virtual screening, J. Med. Chem. 51 (23) (2008) 7442–7448.
[30] D. Wu, Y. Kong, C. Han, J. Chen, L. Hu, H. Jiang, X. Shen, d-Alanine:d-alanine ligase as a new target for the flavonoids quercetin and apigenin, Int. J. Antimicrob. Agents 32 (5) (2008) 421–426.
[31] M. Sova, G. Cadez, S. Turk, V. Majce, S. Polanc, S. Batson, A.J. Lloyd, D.I. Roper, C.W. Fishwick, S. Gobec, Design and synthesis of new hydroxyethylamines as inhibitors of D-alanyl-D-lactate ligase (VanA) and D-alanyl-D-alanine ligase (DdlB), Bioorg. Med. Chem. Lett 19 (5) (2009) 1376–1379.
[32] G. Triola, S. Wetzel, B. Ellinger, M.A. Koch, K. Hubel, D. Rauh, H. Waldmann, ATP competitive inhibitors of D-alanine–D-alanine ligase based on protein kinase inhibitor scaffold, Bioorg. Med. Chem. Lett 17 (2009) 1079–1087.
[33] I. Tytgat, S. Vandevuer, I. Ortmans, F. Sirockin, E. Colacino, F. Van Bambeke, C. Duez, J.H. Poupaert, P.M. Tulkens, A. Dejaegere, M. Prévost, Structure-Based design of benzoxazoles as new inhibitors for D-alanyl-D-alanine ligase, QSAR Comb. Sci. 28 (11–12) (2009) 1394–1404.
[34] B. Vehar, M. Hrast, A. Kovac, J. Konc, K. Mariner, I. Chopra, A.J. O'Neill, D. Janezic, S. Gobec, Ellipticines and 9-acridinylamines as inhibitors of D-alanine:D-alanine ligase, Bioorg. Med. Chem. Lett 19 (2011) 5137–5146.
[35] M. Hrast, B. Vehar, S. Turk, J. Konc, S. Gobec, D. Janezic, Function of the D-alanine:D-alanine ligase lid loop: a molecular modeling and bioactivity study, J. Med. Chem. 55 (15) (2012) 6849–6856.
[36] V. Skedelj, E. Arsovska, T. Tomasic, A. Kroflic, V. Hodnik, M. Hrast, M. Bester-Rogac, G. Anderluh, S. Gobec, J. Bostock, I. Chopra, A.J. O'Neill, C. Randall, A. Zega, 6-Arylpyrido[2,3-d]pyrimidines as novel ATP-competitive inhibitors of bacterial D-alanine:D-alanine ligase, PloS One 7 (8) (2012) e39922.
[37] S. Isik, D. Vullo, S. Durdagi, D. Ekinci, M. Senturk, A. Cetin, E. Senturk, C.T. Supuran, Interaction of carbonic anhydrase isozymes I, II, and IX with some pyridine and phenol hydrazinecarbothioamide derivatives, Bioorg. Med. Chem. Lett 25 (23) (2015) 5636–5641.
[38] A. Paneth, T. Plech, B. Kapron, D. Hagel, U. Kosikowska, E. Kusmierz, K. Dzitko,

P. Paneth, Design, synthesis and biological evaluation of 4-benzoyl-1-dichlorobenzoylthiosemicarbazides as potent Gram-positive antibacterial agents, J. Enzym. Inhib. Med. Chem. (2015) 1–7.
[39] L. Maingot, J. Elbakali, J. Dumont, D. Bosc, N. Cousaert, A. Urban, G. Deglane, B. Villoutreix, H. Nagase, O. Sperandio, F. Leroux, B. Deprez, R. Deprez-Poulain, Aggrecanase-2 inhibitors based on the acylthiosemicarbazide zinc-binding group, Eur. J. Med. Chem. 69C (2013) 244–261.
[40] A. Hasan, N.F. Thomas, S. Gapil, Synthesis, characterization and antifungal evaluation of 5-substituted-4-amino-1,2,4-triazole-3-thioesters, Molecules 16 (2) (2011) 1297–1309.
[41] O.-u.-R. Abid, T.M. Babar, F.I. Ali, S. Ahmed, A. Wadood, N.H. Rama, R. Uddin, H. Zaheer ul, A. Khan, M.I. Choudhary, Identification of novel urease inhibitors by high-throughput virtual and in vitro screening, ACS Med. Chem. Lett. 1 (4) (2010) 145–149.
[42] I. Khan, S. Ali, S. Hameed, N.H. Rama, M.T. Hussain, A. Wadood, R. Uddin, Z. Ul-Haq, A. Khan, S. Ali, M.I. Choudhary, Synthesis, antioxidant activities and urease inhibition of some new 1,2,4-triazole and 1,3,4-thiadiazole derivatives, Eur. J. Med. Chem. 45 (11) (2010) 5200–5207.
[43] S.J. Azhari, M.R. Mlahi, A.A. Al-Asmy, M.M. Mostafa, Synthesis of novel binary and ternary complexes derived from 1-(2-hydroxy benzoyl)-4-phenylthiosemicarbazide (L1) and 2,2′-dipyridyl (L2) with CoII, CuII and ZnII salts, Spectrochim. Acta Mol. Biomol. Spectrosc. 136 (Part B) (2015) 185–191.
[44] J. Boström, A. Hogner, A. Llinàs, E. Wellner, A.T. Plowright, Oxadiazoles in medicinal chemistry, J. Med. Chem. 55 (5) (2012) 1817–1830.
[45] P.A. Lanzetta, L.J. Alvarez, P.S. Reinach, O.A. Candia, An improved assay for nanomole amounts of inorganic phosphate, Anal. Biochem. 100 (1) (1979) 95–97.
[46] B.A. Ellsworth, N.J. Tom, P.A. Bartlett, Synthesis and evaluation of inhibitors of bacterial D-alanine:D-alanine ligases, Chem. Biol. 3 (1) (1996) 37–44.
[47] A.J. Ryan, N.M. Gray, P.N. Lowe, C.-w. Chung, Effect of detergent on "promiscuous" inhibitors, J. Med. Chem. 46 (16) (2003) 3448–3451.
[48] S.L. McGovern, B.T. Helfand, B. Feng, B.K. Shoichet, A specific mechanism of nonspecific inhibition, J. Med. Chem. 46 (20) (2003) 4265–4272.
[49] R.A. Copeland, Evaluation of Enzyme Inhibitors in Drug Discovery: a Guide for Medicinal Chemists and Pharmacologists, second ed. ed, John Wiley & Sons, 2013, p. 572.
[50] Y. Shi, C.T. Walsh, Active site mapping of Escherichia coli D-Ala-D-Ala ligase by structure-based mutagenesis, Biochemistry 34 (9) (1995) 2768–2776.
[51] M.-L. Foucault, F. Depardieu, P. Courvalin, C. Grillot-Courvalin, Inducible expression eliminates the fitness cost of vancomycin resistance in enterococci, Proc. Natl. Acad. Sci. U.S.A. 107 (39) (2010) 16964–16969.
[52] F. Van Bambeke, M. Chauvel, P.E. Reynolds, H.S. Fraimow, P. Courvalin, Vancomycin-Dependent Enterococcus faecalis clinical isolates and revertant mutants, Antimicrob. Agents Chemother. 43 (1) (1999) 41–47.
[53] L. Abadía-Patiño, K. Christiansen, J. Bell, P. Courvalin, B. Périchon, VanE-Type vancomycin-resistant Enterococcus faecalis clinical isolates from Australia, Antimicrob. Agents Chemother. 48 (12) (2004) 4882–4885.
[54] S. Tsiodras, H.S. Gold, G. Sakoulas, G.M. Eliopoulos, C. Wennersten, L. Venkataraman, R.C. Moellering Jr., M.J. Ferraro, Linezolid resistance in a clinical isolate of Staphylococcus aureus, Lancet 358 (9277) (2001) 207–208.
[55] T. Plech, M. Wujec, A. Siwek, U. Kosikowska, A. Malm, Synthesis and antimicrobial activity of thiosemicarbazides, s-triazoles and their Mannich bases bearing 3-chlorophenyl moiety, Eur. J. Med. Chem. 46 (1) (2011) 241–248.
[56] A. Paneth, T. Plech, B. Kapron, D. Hagel, U. Kosikowska, E. Kusmierz, K. Dzitko, P. Paneth, Design, synthesis and biological evaluation of 4-benzoyl-1-dichlorobenzoylthiosemicarbazides as potent Gram-positive antibacterial agents, J. Enzym. Inhib. Med. Chem. 31 (3) (2016) 434–440.
[57] T. Plech, A. Paneth, B. Kapron, U. Kosikowska, A. Malm, A. Strzelczyk, P. Staczek, Structure-activity relationship studies of microbiologically active thiosemicarbazides derived from hydroxybenzoic acid hydrazides, Chem. Biol. Drug Des. 85 (3) (2015) 315–325.
[58] A. Siwek, P. Stączek, M. Wujec, J. Stefańska, U. Kosikowska, A. Malm, S. Jankowski, P. Paneth, Biological and docking studies of topoisomerase IV inhibition by thiosemicarbazides, J. Mol. Model. 17 (9) (2011) 2297–2303.
[59] D. Jamindar, W.G. Gutheil, A liquid chromatography–tandem mass spectrometry assay for Marfey's derivatives of l-Ala, d-Ala, and d-Ala-d-Ala: application to the in vivo confirmation of alanine racemase as the target of cycloserine in Escherichia coli, Anal. Biochem. 396 (1) (2010) 1–7.
[60] H. Vemula, N.J. Ayon, W.G. Gutheil, Cytoplasmic peptidoglycan intermediate levels in Staphylococcus aureus, Biochimie 121 (2016) 72–78.
[61] R. Bhushan, H. Brückner, Marfey's reagent for chiral amino acid analysis: a review, Amino Acids 27 (3–4) (2004) 231–247.
[62] P. Ertl, B. Rohde, P. Selzer, Fast calculation of molecular polar surface area as a sum of fragment-based contributions and its application to the prediction of drug transport properties, J. Med. Chem. 43 (20) (2000) 3714–3717.
[63] J.D. Hughes, J. Blagg, D.A. Price, S. Bailey, G.A. Decrescenzo, R.V. Devraj, E. Ellsworth, Y.M. Fobian, M.E. Gibbs, R.W. Gilles, N. Greene, E. Huang, T. Krieger-Burke, J. Loesel, T. Wager, L. Whiteley, Y. Zhang, Physiochemical drug properties associated with in vivo toxicological outcomes, Bioorg. Med. Chem. Lett 18 (17) (2008) 4872–4875.
[64] D.F. Veber, S.R. Johnson, H.Y. Cheng, B.R. Smith, K.W. Ward, K.D. Kopple, Molecular properties that influence the oral bioavailability of drug candidates, J. Med. Chem. 45 (12) (2002) 2615–2623.
[65] K.M. Khan, M. Rasheed, Z. Ullah, S. Hayat, F. Kaukab, M.I. Choudhary, A. ur-Rahman, S. Perveen, Synthesis and in vitro leishmanicidal activity of some hydrazides and their analogues, Bioorg. Med. Chem. 11 (7) (2003) 1381–1387.
[66] C. Runti, F. Collino, Thiosemicarbazide derivatives with tuberculostatic activity, Boll. Chim. Farm. 100 (1961) 837–845.
[67] E. Hoggarth, 251 Compounds related to thiosemicarbazide. Part II. 1-Benzoylthiosemicarbazides, J. Chem. Soc. (0) (1949) 1163–1167.
[68] S. Suresh, K.I. Bhat, P.C. Jalihal, K. Basavaraj, Synthesis and antimicrobial activity of some new 2,5 disubstituted 1,3,4-thiadiazoles, J. Chem. Pharmaceut. Sci. 2 (2) (2009) 141–145.
[69] D.-S. Guo, Synthesis and antibacterial activities of 2-benzoyl-N-aryl hydrazinecarboxamides, You Ji Hua Xue 24 (9) (2004) 1118–1121.
[70] G. Sheldrick, Crystal structure refinement with SHELXL, Acta Crystallogr. C 71 (1) (2015) 3–8.
[71] A.L.P.L.A.T.O.N. Spek, A Multipurpose Crystallographic Tool, Utrecht Univeristy, Utrecht (The Netherlands), 2005.
[72] A.E. Jacob, S.J. Hobbs, Conjugal transfer of plasmid-borne multiple antibiotic resistance in Streptococcus faecalis var. zymogenes, J. Bacteriol. 117 (2) (1974) 360–372.
[73] C. Le Bouguénec, G. de Cespédès, T. Horaud, Presence of chromosomal elements resembling the composite structure Tn3701 in streptococci, J. Bacteriol. 172 (2) (1990) 727–734.
[74] L.M. Guzman, D. Belin, M.J. Carson, J. Beckwith, Tight regulation, modulation, and high-level expression by vectors containing the arabinose PBAD promoter, J. Bacteriol. 177 (14) (1995) 4121–4130.
[75] J.M. Fleckenstein, K. Roy, J.F. Fischer, M. Burkitt, Identification of a two-partner secretion locus of enterotoxigenic Escherichia coli, Infect. Immun. 74 (4) (2006) 2245–2258.
[76] G.A. Gambetta, J.C. Lagarias, Genetic engineering of phytochrome biosynthesis in bacteria, Proc. Natl. Acad. Sci. U.S.A. 98 (19) (2001) 10566–10571.
[77] U.K. Laemmli, Cleavage of structural proteins during the assembly of the head of bacteriophage T4, Nature 227 (5259) (1970) 680–685.
[78] J. Mortier, J.R.C. Prévost, D. Sydow, S. Teuchert, C. Omieczynski, M. Bermudez, R. Frédérick, G. Wolber, Arginase structure and inhibition: catalytic site plasticity reveals new modulation possibilities, Sci. Rep. 7 (2017), 13616.
[79] O. Takikawa, T. Kuroiwa, F. Yamazaki, R. Kido, Mechanism of interferon-gamma action. Characterization of indoleamine 2,3-dioxygenase in cultured human cells induced by interferon-gamma and evaluation of the enzyme-mediated tryptophan degradation in its anticellular activity, J. Biol. Chem. 263 (4) (1988) 2041–2048.
[80] R.A. Ward, C. Brassington, A.L. Breeze, A. Caputo, S. Critchlow, G. Davies, L. Goodwin, G. Hassall, R. Greenwood, G.A. Holdgate, M. Mrosek, R.A. Norman, S. Pearson, J. Tart, J.A. Tucker, M. Vogtherr, D. Whittaker, J. Wingfield, J. Winter, K. Hudson, Design and synthesis of novel lactate dehydrogenase a inhibitors by fragment-based lead generation, J. Med. Chem. 55 (7) (2012) 3285–3306.
[81] G. Labar, C. Bauvois, G.G. Muccioli, J. Wouters, D.M. Lambert, Disulfiram is an inhibitor of human purified monoacylglycerol lipase, the enzyme regulating 2-arachidonoylglycerol signaling, Chembiochem 8 (11) (2007) 1293–1297.
[82] S. Ravez, C. Corbet, Q. Spillier, A. Dutu, A.D. Robin, E. Mullarky, L.C. Cantley, O. Feron, R. Frédérick, α-Ketothioamide derivatives: a promising tool to interrogate phosphoglycerate dehydrogenase (PHGDH), J. Med. Chem. 60 (4) (2017) 1591–1597.
[83] H. Brückner, C. Gah, High-performance liquid chromatographic separation of dl-amino acids derivatized with chiral variants of Sanger's reagent, J. Chromatogr. A 555 (1–2) (1991) 81–95.
[84] Methods for Dilution Antimicrobial Susceptibility Tests for Bacteria that Grow Aerobically, Approved Standard-ninth Edition, Clinical and Laboratory Standards Institute, Wayne, PA, vol. 32, No. 2, M07-A9, 2012.
[85] Methods for Determining Bactericidal Activity of Antimicrobial Agents, Approved Guidelines, Clinical and Laboratory Standards Institute, Wayne, PA, vol. 19, No. 18, M26-A, 1999.
[86] W. Strober, Trypan blue exclusion test of cell viability, Curr. Protoc. Im. 21 (1) (2001). Appendix 3, Appendix 3B.
[87] S. Tsuchiya, M. Yamabe, Y. Yamaguchi, Y. Kobayashi, T. Konno, K. Tada, Establishment and characterization of a human acute monocytic leukemia cell line (THP-1), Int. J. Canc. 26 (2) (1980) 171–176.
[88] B. Scorneaux, Y. Ouadrhiri, G. Anzalone, P.M. Tulkens, Effect of recombinant human gamma interferon on intracellular activities of antibiotics against Listeria monocytogenes in the human macrophage cell line THP-1, Antimicrob. Agents Chemother. 40 (5) (1996) 1225–1230.